Artificial-Delay Adaptive Control for Under-actuated Euler-Lagrange Robotics

Roy, Spandan; Baldi, Simone; Li, Peng; Narayanan, Viswa

DOI
10.1109/TMECH.2021.3052068

Publication date
2021

Document Version
Accepted author manuscript

Published in
IEEE/ASME Transactions on Mechatronics

Artificial-Delay Adaptive Control for Under-actuated Euler-Lagrange Robotics

Spandan Roy, Simone Baldi, Peng Li and Viswa N. Sankaranarayanan

***Abstract*—Artificial-delay control is a method in which state and input measurements collected at an immediate past time instant (i.e. artificially delayed) are used to compensate the uncertain dynamics affecting the system at the current time. This work formulates an artificial-delay control method with adaptive gains in the presence of nonlinear (Euler-Lagrange) under-actuation. The appeal of studying Euler-Lagrange dynamics is to capture many robotics applications of practical interest, as demonstrated via stability and robustness analysis and via robotic ship and robotic aerial vehicle test cases.**

***Index Terms*—Under-actuated robotics, artificial-delay control, time delay estimation, Euler-Lagrange systems.**

I. Introduction

The method of *artificial-delay control* was formulated as a control scheme with reduced a priori knowledge of the system dynamics [1]–[3]. The main idea of artificial-delay control is to use state and input measurements collected at an immediate past time instant (i.e. with an artificial delay) to compensate the uncertain system dynamics affecting the system at the current time instant. Artificial-delay control is also known in literature as *time-delay control*: because this terminology can be confused with the field of control of time-delay systems, we use 'artificial-delay control' throughout this work.

Its simple design made artificial-delay control appealing over the years, up to recent results based on linear matrix inequalities [4], [5] that showed stability of an artificial-delay closed-loop system under fast enough sampling (i.e. with small artificial delay). Besides delayed state and input measurements, artificial-delay control also requires a robustifying control term to counteract the error arising from compensating the dynamics at the current time instant with past measurements. This error is known as time-delay estimation (TDE) error. The robustifying term can use an upper bound of the TDE error or an online estimated bound [6]–[8]. Both constant and state-dependent bounds have been proposed. Adaptive control methods proposed to estimate online the effect of the TDE error offered a perspective to TDE-based control with limited structural knowledge, since the knowledge of upper bounds to the uncertainty is not required to design the controller and the uncertainty does not have to be assumed bounded a priori.

The first two authors equally contributed to the work. This work is supported by the Natural Science Foundation of China grant no. 62073074, and by the special guiding fund for double first-class grant no. 3307012001A (corresponding author: S. Baldi).

S. Roy and V. N. Sankaranarayanan are with Robotics Research Centre, International Institute of Information Technology Hyderabad, India e-mails: spandan.roy@iiit.ac.in, viswa.narayanan@research.iiit.ac.in

S. Baldi is with School of Cyber Science and Engineering, Southeast University, Nanjing, China, and guest with Delft Center for System and Control, Delft University of Technology, The Netherlands e-mail: s.baldi@tudelft.nl

P. Li is with School of Cyber Science and Engineering, Southeast University, Nanjing, China e-mail: lpeng_2013@163.com

Artificial-delay control has been widely applied in Euler-Lagrange robotics, such as manipulators [9]–[12], exoskeleton or bipedal robots [8], [13], actuators [14], [15], cranes [16], [17], excavators [18] and mobile platforms [19], [20]. Despite the heterogeneity of the applications, the underlying artificial-delay design is similar, which shows its flexibility to different Euler-Lagrange system structures. Stability and robustness analysis of artificial-delay control typically rely on the dynamics being fully-actuated: a notable exception are the under-actuated TDE-based approaches appeared for electric motors [21], [22], requiring linear dynamics and knowledge of upper bounds to the uncertainty. This opens the question of finding an artificial-delay control method for under-actuated Euler-Lagrange robotics, as well as embedding this method with adaptation capabilities.

Because of the reduced number of actuators, under-actuation in robotic systems has advantages in terms of lightweight, energy consumption and system simplicity. Under-actuated robotics encompass tower [23], [24] and offshore cranes [25], [26], robotic aerial [27], marine [28], [29] and ground vehicles [30], robotic hands [31], and many more. Control of under-actuated systems is more challenging than the corresponding fully-actuated version. As a result, state-of-the-art controllers for under-actuated systems are tailored to specific structures or assumptions (e.g. linear structure, mass matrix depending on a limited set of variables, state derivatives or unactuated states being bounded [21], [22], [32]–[36]). The resulting design is effective for the system at hand, but not flexible for other structures. Also backstepping (or adaptive backstepping) approaches have been deeply investigated (cf. [37]–[40] and references therein): this paradigm is quite flexible for controlling a wide range of robotic systems, provided that structural knowledge is available for selecting the uncertainties in standard linear-in-the-parameter form. While this is possible in many applications (sometimes inner/outer loop architectures are used to make this possible [41], [42]), it is a different philosophy than artificial-delay control, where the TDE mechanism is indeed used to limit the structural knowledge.

This work gives an answer to control with limited structural knowledge of under-actuated systems in the framework of artificial-delay control. The contributions of the work are:

- To formulate the artificial-delay design so as to include under-actuated dynamics in the TDE compensation, without relying on linearity, structure of the mass matrix nor boundedness of state derivatives or unactuated states;
- To retain the properties of adaptive designs, where instead of upper bounding a priori the TDE error as in robust design, the effect of the TDE error is estimated on-line;
- To demonstrate the flexibility of the proposed artificial-

delay framework analytically and by testing it in systems with different structures (robotic ship and aerial vehicle).

The rest of the paper is organized as follows: Sect. II provides the problem formulation; Sect. III covers the control design with stability/robustness analysis in Sect. IV; test cases are in Sect. V and VI with conclusions in Sect. VII.

II. System Dynamics and Problem Formulation

Consider the following class of under-actuated Euler-Lagrange (EL) systems

$$\mathbf{M}(\mathbf{q})\ddot{\mathbf{q}} + \mathbf{C}(\mathbf{q},\dot{\mathbf{q}})\dot{\mathbf{q}} + \mathbf{G}(\mathbf{q}) + \mathbf{F}(\dot{\mathbf{q}}) + \mathbf{d_s} = [\boldsymbol{\tau}^T \ \mathbf{0}^T]^T, \quad (1)$$

where $\mathbf{q} \in \mathbb{R}^n$ is the system state; $\mathbf{M}(\mathbf{q}) \in \mathbb{R}^{n\times n}$ is the mass matrix (containing mass and inertia terms); $\mathbf{C}(\mathbf{q},\dot{\mathbf{q}}) \in \mathbb{R}^{n\times n}$ denotes the Coriolis, centripetal terms, which are proportional to velocity; $\mathbf{G}(\mathbf{q}) \in \mathbb{R}^n$ denotes the gravity forces; $\mathbf{F}(\dot{\mathbf{q}}) \in \mathbb{R}^n$ denotes velocity-dependent damping and friction forces; $\mathbf{d_s}(t) \in \mathbb{R}^n$ denotes bounded external disturbance and $\boldsymbol{\tau} \in \mathbb{R}^m$ is the control input where $(n-m) \leq m < n$.

The interested reader can check [25]–[31] and references therein to see how (1) apply to many under-actuated robotic systems spanning from cranes to vehicles, or to standard benchmarks such as cart-poles and Acrobots. For such EL systems of practical interest, (1) exhibits a few properties, later exploited for control design and stability analysis:

Property 1: $\exists c_b, g_b, f_b, \overline{d} \in \mathbb{R}^+$ such that $||\mathbf{C}(\mathbf{q},\dot{\mathbf{q}})|| \leq c_b||\dot{\mathbf{q}}||$, $||\mathbf{G}(\mathbf{q})|| \leq g_b$, $||\mathbf{F}(\dot{\mathbf{q}})|| \leq f_b||\dot{\mathbf{q}}||$ and $||\mathbf{d_s}(t)|| \leq \overline{d}$.

Property 2: The matrix $\mathbf{M}(\mathbf{q})$ is uniformly positive definite. This implies that $\exists \mu_1, \mu_2 \in \mathbb{R}^+$ such that

$$0 < \mu_1\mathbf{I} \leq \mathbf{M}(\mathbf{q}) \leq \mu_2\mathbf{I}. \quad (2)$$

Let $\mathbf{M}$ be decomposed as $\mathbf{M} \triangleq \hat{\mathbf{M}} + \Delta\mathbf{M}$, where $\hat{\mathbf{M}}$ and $\Delta\mathbf{M}$ represent the nominal and perturbation terms of $\mathbf{M}$, respectively. The EL system (1) is considered to be uncertain in the sense that precise knowledge of the system dynamics terms $\mathbf{M}, \mathbf{C}, \mathbf{F}, \mathbf{G}$ and $\mathbf{d_s}$ is not available. In particular, the following challenge is imposed in the form of an assumption:

Assumption 1. *Only the knowledge of $\hat{\mathbf{M}}$ and an upper bound for $\Delta\mathbf{M}$ are available; the terms $\mathbf{C}, \mathbf{F}, \mathbf{G}$ and $\mathbf{d_s}$ (and their upper bounds c_b, f_b, g_b and $\overline{d}$) are considered to be unknown.*

Remark 1 (No structure-specific assumptions)**.** *Under-actuated designs from literature require either linear structure, or the mass matrix to depend on a limited set of variables, or the state derivatives/unactuated states to be bounded [21], [32]–[35]. Here, no assumption is made on how actuated and unactuated states affect the dynamics terms $\mathbf{M}, \mathbf{C}, \mathbf{F}, \mathbf{G}$.*

For controller design, as well as for convenience of notation, let us rewrite system (1) by distinguishing between the actuated and unactuated subsystems, as follows:

$$\mathbf{M}(\mathbf{q})\ddot{\mathbf{q}} + \mathbf{N}(\mathbf{q},\dot{\mathbf{q}}) + \mathbf{d_s} = [\boldsymbol{\tau}^T \ \mathbf{0}^T]^T, \quad (3)$$

where $\mathbf{q} = [\mathbf{q_a}^T \ \mathbf{q_u}^T]^T, \mathbf{q_a} \in \mathbb{R}^m, \mathbf{q_u} \in \mathbb{R}^{(n-m)}$

$$\mathbf{M} \triangleq \begin{bmatrix} \mathbf{M_{aa}} & \mathbf{M_{au}} \\ \mathbf{M_{ua}} & \mathbf{M_{uu}} \end{bmatrix},$$

$$\mathbf{N} \triangleq \mathbf{C}\dot{\mathbf{q}} + \mathbf{G} + \mathbf{F} = \begin{bmatrix} \mathbf{N_a}^T & \mathbf{N_u}^T \end{bmatrix}^T,$$

$$\mathbf{d_s} \triangleq \begin{bmatrix} \mathbf{d_a}^T & \mathbf{d_u}^T \end{bmatrix}^T, \mathbf{d_a} \in \mathbb{R}^m, \mathbf{d_u} \in \mathbb{R}^{(n-m)}, \quad (4)$$

with $\mathbf{q_a}$ and $\mathbf{q_u}$ being actuated and unactuated states, respectively. System dynamics (3) can be rearranged as

$$\mathbf{M_{uu}}\ddot{\mathbf{q}}_\mathbf{u} = -\mathbf{M_{ua}}\ddot{\mathbf{q}}_\mathbf{a} + \mathbf{h_u}, \quad (5a)$$

$$\mathbf{M_s}\ddot{\mathbf{q}}_\mathbf{a} = \boldsymbol{\tau} + \mathbf{h_a}, \quad (5b)$$

where $\mathbf{h_u} \triangleq -(\mathbf{N_u} + \mathbf{d_u})$,

$\mathbf{h_a} \triangleq -(\mathbf{N_a} + \mathbf{d_a} - \mathbf{M_{au}}\mathbf{M_{uu}}^{-1}(\mathbf{N_u} + \mathbf{d_u}))$,

$\mathbf{M_s} \triangleq \mathbf{M_{aa}} - \mathbf{M_{au}}\mathbf{M_{uu}}^{-1}\mathbf{M_{ua}}$.

As $\mathbf{M} > \mathbf{0}$ by *Property 2*, existence of $\mathbf{M_s}^{-1}, \mathbf{M_{aa}}^{-1}$ and $\mathbf{M_{uu}}^{-1}$ is ensured.

III. Controller Design

Let us consider the tracking of a desired trajectory $\mathbf{q}^d(t)$ such that $\mathbf{q}^d, \dot{\mathbf{q}}^d, \ddot{\mathbf{q}}^d$ are bounded. Let $\mathbf{q}^d(t) \triangleq [\mathbf{q_a^d}^T \ \mathbf{q_u^d}^T]^T$ and let $\mathbf{e_a}(t) \triangleq \mathbf{q}_a(t) - \mathbf{q_a^d}(t)$ and $\mathbf{e_u}(t) \triangleq \mathbf{q}_u(t) - \mathbf{q_u^d}(t)$ be the tracking error in the actuated and unactuated subsystems, respectively. The actuated subsystem (5b) can be written as

$$\begin{aligned} \overline{\mathbf{M}}_\mathbf{a}\ddot{\mathbf{q}}_\mathbf{a} + (\mathbf{M_s} - \overline{\mathbf{M}}_a)\ddot{\mathbf{q}}_\mathbf{a} - \mathbf{h_a} &= \boldsymbol{\tau} \\ \Rightarrow \overline{\mathbf{M}}_\mathbf{a}\ddot{\mathbf{q}}_\mathbf{a} + \overline{\mathbf{h}}_\mathbf{a} &= \boldsymbol{\tau}, \end{aligned} \quad (6)$$

where $\overline{\mathbf{h}}_\mathbf{a} \triangleq (\mathbf{M_s} - \overline{\mathbf{M}}_\mathbf{a})\ddot{\mathbf{q}}_\mathbf{a} - \mathbf{h_a}$, and $\overline{\mathbf{M}}_\mathbf{a}$ is a user-defined positive definite matrix whose choice will be discussed later (cf. Lemma 1). The control input $\boldsymbol{\tau}$ is designed as

$$\boldsymbol{\tau} = \overline{\mathbf{M}}_\mathbf{a}\boldsymbol{\nu} + \hat{\overline{\mathbf{h}}}_\mathbf{a}, \quad (7a)$$

$$\hat{\overline{\mathbf{h}}}_\mathbf{a} = (\boldsymbol{\tau})_L - \overline{\mathbf{M}}_\mathbf{a}(\ddot{\mathbf{q}}_\mathbf{a})_L. \quad (7b)$$

$$\boldsymbol{\nu} = \ddot{\mathbf{q}}_\mathbf{a}^d - \mathbf{K_{Da}}\dot{\mathbf{e}}_\mathbf{a} - \mathbf{K_{Pa}}\mathbf{e_a} - \mathbf{K_{Du}}\dot{\mathbf{e}}_\mathbf{u} - \mathbf{K_{Pu}}\mathbf{e_u} - \Delta\boldsymbol{\tau},$$

$$\Delta\boldsymbol{\tau} = \begin{cases} \rho\frac{\mathbf{r}}{||\mathbf{r}||} & \text{if } ||\mathbf{r}|| \geq \epsilon \\ \rho\frac{\mathbf{r}}{\epsilon} & \text{if } ||\mathbf{r}|| < \epsilon \end{cases}, \ \mathbf{r} = \mathbf{B}^T\mathbf{P_a}\boldsymbol{\xi}_\mathbf{a}, \ \boldsymbol{\xi}_\mathbf{a} \triangleq \begin{bmatrix} \mathbf{e_a} \\ \dot{\mathbf{e}}_\mathbf{a} \end{bmatrix}, \quad (7c)$$

where $(\cdot)_L = (\cdot)(t-L)$ denotes a delayed version of the signal with artificial delay L; $\mathbf{K_{Da}}, \mathbf{K_{Pa}} \in \mathbb{R}^{m\times m}$ and $\mathbf{K_{Du}}, \mathbf{K_{Pu}} \in \mathbb{R}^{m\times(n-m)}$ are user-defined matrices such that $\mathbf{K_{Da}} > \mathbf{0}, \mathbf{K_{Pa}} > \mathbf{0}$ and $\mathbf{K_{Du}}, \mathbf{K_{Pu}}$ are of full rank $(n-m)$; ρ is a robustifying gain which will be designed later (cf. (19)); $\epsilon > 0$ is a scalar whose role it to avoid discontinuity in control input by pushing the error towards a boundary layer; $\mathbf{P_a} > \mathbf{0}$ is the solution to the Lyapunov equation

$$\mathbf{A_a}^T\mathbf{P_a} + \mathbf{P_a}\mathbf{A_a} = -\mathbf{Q_a},$$

$$\mathbf{A_a} \triangleq \begin{bmatrix} \mathbf{0} & \mathbf{I} \\ -\mathbf{K_{Pa}} & -\mathbf{K_{Da}} \end{bmatrix}, \ \mathbf{B} \triangleq \begin{bmatrix} \mathbf{0} \\ \mathbf{I} \end{bmatrix}, \ \mathbf{Q_a} > \mathbf{0}.$$

Note that as the gains $\mathbf{K_{Pa}}$ and $\mathbf{K_{Da}}$ are positive definite by design, $\mathbf{A_a}$ is guaranteed to be Hurwitz.

Remark 2 (Structural knowledge)**.** *The use of $\hat{\overline{\mathbf{h}}}_\mathbf{a}$ in (7a), implies that delayed input and state are used to compensate system dynamics at the current time instant. The notable feature of such mechanism is that it is independent of structural or parametric knowledge of $\overline{\mathbf{h}}_\mathbf{a}$, in line with Assumption 1. The delayed state also include acceleration feedback, which is not a peculiarity of our design, but it is standard in artificial-delay literature*[1] *[1]–[3].*

[1]Acceleration feedback via inertial measurement units has become quite standard, and several works in this sense regularly appear in robotics literature [10], [13], [19], [43], [44].

Substituting (7a) into (6), error dynamics for the actuated subsystem is obtained as

$$\begin{aligned}\ddot{\mathbf{e}}_\mathbf{a} &= -\mathbf{K_{Da}}\dot{\mathbf{e}}_\mathbf{a} - \mathbf{K_{Pa}}\mathbf{e_a} - \mathbf{K_{Du}}\dot{\mathbf{e}}_\mathbf{u} - \mathbf{K_{Pu}}\mathbf{e_u} - \Delta\boldsymbol{\tau} + \boldsymbol{\sigma_a}\\ \dot{\boldsymbol{\xi}}_\mathbf{a} &= \mathbf{A_a}\boldsymbol{\xi_a} + \mathbf{B}(-\Delta\boldsymbol{\tau} + \boldsymbol{\sigma_a} - \mathbf{K_{Du}}\dot{\mathbf{e}}_\mathbf{u} - \mathbf{K_{Pu}}\mathbf{e_u})\\ &= \mathbf{A_a}\boldsymbol{\xi_a} + \mathbf{B}(-\Delta\boldsymbol{\tau} + \boldsymbol{\phi}_1), \end{aligned} \tag{8}$$

where $\boldsymbol{\sigma_a} \triangleq \overline{\mathbf{M}}_\mathbf{a}^{-1}(\hat{\mathbf{h}}_\mathbf{a} - \overline{\mathbf{h}}_\mathbf{a})$, $\boldsymbol{\phi}_1 \triangleq \boldsymbol{\sigma_a} - \mathbf{K_{Du}}\dot{\mathbf{e}}_\mathbf{u} - \mathbf{K_{Pu}}\mathbf{e_u}$. Here $\boldsymbol{\sigma_a}$ is termed as the *TDE error*. We now prove that the TDE error holds an upper-bound structure.

Lemma 1. *The TDE error $\boldsymbol{\sigma_a}$ can be upper bounded as*

$$||\boldsymbol{\sigma_a}|| \leq \theta_0 + \theta_1||\boldsymbol{\xi}||, \tag{9}$$

for unknown positive scalars θ_0, θ_1, with $\boldsymbol{\xi} \triangleq [\mathbf{e}_\mathbf{a}^T\ \mathbf{e}_\mathbf{u}^T\ \dot{\mathbf{e}}_\mathbf{a}^T\ \dot{\mathbf{e}}_\mathbf{u}^T]^T$, provided that the matrix $\overline{\mathbf{M}}_\mathbf{a}$ is selected to satisfy

$$||\mathbf{I} - \mathbf{M_s}^{-1}\overline{\mathbf{M}}_\mathbf{a}|| = \varsigma < 1. \tag{10}$$

Proof. See Appendix. □

Remark 3 (Under-actuated TDE error)**.** *Condition (10) requires $\overline{\mathbf{M}}_\mathbf{a}$ to be not too far from $\mathbf{M_s}$ (note that $\varsigma = 0$ in case $\overline{\mathbf{M}}_\mathbf{a} = \mathbf{M_s}$). In this sense, $\overline{\mathbf{M}}_\mathbf{a}$ in (10) plays the role of a nominal (estimated) mass matrix, a condition also known in conventional TDE methods for fully-actuated systems [1]–[3]. Also note that, as compared to state-dependent structures proposed for full actuation [7], the dependence of θ_0, θ_1 in* (9) *on the system dynamics is different due to under-actuation.*

Following (9) and, the facts $||\boldsymbol{\xi}|| \geq \dot{\mathbf{e}}_\mathbf{u}$ and $||\boldsymbol{\xi}|| \geq \mathbf{e_u}$, the following upper bound on $\boldsymbol{\phi}_1$ in (8) can be derived

$$||\boldsymbol{\phi}_1|| \leq \theta_0^* + \theta_1^*||\boldsymbol{\xi}||, \tag{11}$$

where we define two unknown scalars $\theta_0^* \triangleq \theta_0, \theta_1^* \triangleq \theta_0 + ||\mathbf{K_{Pa}}|| + ||\mathbf{K_{Da}}||$. Further, (8) and (9) reveal that the error dynamics as well as the TDE-error depend explicitly on the unactuated states. Hence, boundedness of (8) cannot be ensured by following/applying state-of-the-art TDE-based methods to actuated subsystem (6) alone.

Using (5a) and (6), the error dynamics of the unactuated subsystem can be represented as

$$\begin{aligned}\ddot{\mathbf{e}}_\mathbf{u} &= \ddot{\mathbf{q}}_\mathbf{u} - \ddot{\mathbf{q}}_\mathbf{u}^d = -\mathbf{M_{uu}}^{-1}\mathbf{M_{ua}}\ddot{\mathbf{q}}_\mathbf{a} + \mathbf{M_{uu}}^{-1}\mathbf{h_u} - \ddot{\mathbf{q}}_\mathbf{u}^d\\ &= -\mathbf{M_{uu}}^{-1}\mathbf{M_{ua}}\overline{\mathbf{M}}_\mathbf{a}^{-1}(\boldsymbol{\tau} - \overline{\mathbf{h}}_\mathbf{a}) + \mathbf{M_{uu}}^{-1}\mathbf{h_u} - \ddot{\mathbf{q}}_\mathbf{u}^d. \end{aligned} \tag{12}$$

Substituting (7a) into (12) and using the relation $\boldsymbol{\sigma_a} = \overline{\mathbf{M}}_\mathbf{a}^{-1}(\hat{\mathbf{h}}_\mathbf{a} - \overline{\mathbf{h}}_\mathbf{a})$ yields

$$\ddot{\mathbf{e}}_\mathbf{u} = -\boldsymbol{\Gamma\nu} + \boldsymbol{\phi}_2, \tag{13}$$

where $\boldsymbol{\Gamma} \triangleq \mathbf{M_{uu}}^{-1}\mathbf{M_{ua}}$, $\boldsymbol{\phi}_2 \triangleq -\boldsymbol{\Gamma\sigma_a} + \mathbf{M_{uu}}^{-1}\mathbf{h_u} - \ddot{\mathbf{q}}_\mathbf{u}^d$.

Note that $(n-m) \leq m$ by the system definition (1); thus, one can design a constant full rank matrix $\mathbf{H} \in \mathbb{R}^{(n-m)\times m}$ such that the following holds:

$$\mathbf{K}_1 \triangleq \mathbf{HK_{Pu}} > \mathbf{0},\ \mathbf{K}_2 \triangleq \mathbf{HK_{Du}} > \mathbf{0}. \tag{14}$$

Adding and subtracting $\mathbf{H}\boldsymbol{\nu}$ to (13) and expanding $\boldsymbol{\nu}$ yields

$$\ddot{\mathbf{e}}_\mathbf{u} = -\mathbf{K}_1\mathbf{e_u} - \mathbf{K}_2\dot{\mathbf{e}}_\mathbf{u} + \boldsymbol{\Gamma\Delta\tau} + \overline{\boldsymbol{\phi}}_2, \tag{15}$$

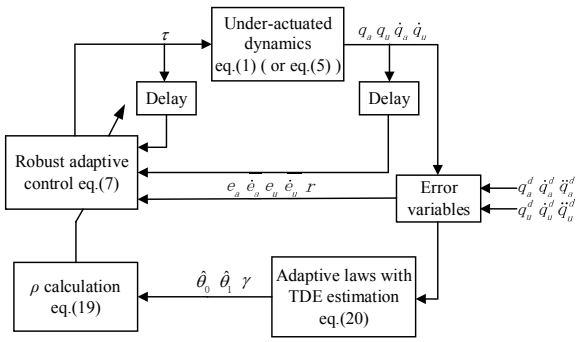

Figure 1. Block diagram of the proposed control scheme.

where $\overline{\boldsymbol{\phi}}_2 \triangleq (\mathbf{H}+\boldsymbol{\Gamma})(\mathbf{K_{Da}}\dot{\mathbf{e}}_\mathbf{a}+\mathbf{K_{Pa}}\mathbf{e_a}+\mathbf{K_{Du}}\dot{\mathbf{e}}_\mathbf{u}+\mathbf{K_{Pu}}\mathbf{e_u}) + \boldsymbol{\phi}_2 - \mathbf{H}(\mathbf{K_{Da}}\dot{\mathbf{e}}_\mathbf{a} + \mathbf{K_{Pa}}\mathbf{e_a})$. Therefore, taking

$$\boldsymbol{\xi}_\mathbf{u} \triangleq [\mathbf{e}_\mathbf{u}^T\ \dot{\mathbf{e}}_\mathbf{u}^T]^T,\ \mathbf{A_u} \triangleq \begin{bmatrix}\mathbf{0} & \mathbf{I}\\ -\mathbf{K}_1 & -\mathbf{K}_2\end{bmatrix},$$

the error dynamics (15) can be represented as

$$\dot{\boldsymbol{\xi}}_\mathbf{u} = \mathbf{A_u}\boldsymbol{\xi_u} + \mathbf{B}(\boldsymbol{\Gamma\Delta\tau} + \overline{\boldsymbol{\phi}}_2). \tag{16}$$

Design of $\mathbf{K}_1 > \mathbf{0}, \mathbf{K}_2 > \mathbf{0}$ guarantees that $\mathbf{A_u}$ is Hurwitz.

Using Property 1, the following holds for the term $\mathbf{N}$ in (3):

$$||\mathbf{N_u}|| \leq ||\mathbf{N}|| \leq g_b + f_b||\mathbf{x}|| + c_b||\mathbf{x}||^2, \tag{17}$$

where $\mathbf{x} \triangleq [\mathbf{q}^T\ \dot{\mathbf{q}}^T]^T$. Now, observing the structures of $\mathbf{h_u}$, $\boldsymbol{\phi}_2, \overline{\boldsymbol{\phi}}_2$ in (5a), (13) and (15) respectively, and using the relation (17), the following upper bound on $\overline{\boldsymbol{\phi}}_2$ can be derived

$$||\overline{\boldsymbol{\phi}}_2||||\mathbf{P_uB}|| \leq \theta_0^{**} + \theta_1^{**}||\boldsymbol{\xi}|| + \theta_2^{**}||\boldsymbol{\xi}||^2, \tag{18}$$

where $\theta_i^{**} \in \mathbb{R}^+$, $i = 0, 1, 2$ are unknown scalars (cf. Assumption 1); $\mathbf{P_u} > \mathbf{0}$ is the solution to the Lyapunov equation $\mathbf{A_u}^T\mathbf{P_u} + \mathbf{P_u}\mathbf{A_u} = -\mathbf{Q_u}$ for some $\mathbf{Q_u} > \mathbf{0}$. The term $||\mathbf{P_uB}||$ is solely considered in (18) for subsequent mathematical simplifications. Note that while deriving the relation (18), the following relations are utilized: $\boldsymbol{\xi} = \mathbf{x} - \begin{bmatrix}\mathbf{q}^d\\ \dot{\mathbf{q}}^d\end{bmatrix}$ and $\mathbf{q}^d, \dot{\mathbf{q}}^d$ are bounded by design.

Observing the upper bound structures of $||\boldsymbol{\phi}_1||$ and $||\overline{\boldsymbol{\phi}}_2||$ in (11) and (18) respectively, the gain ρ in (7c) is designed as

$$\rho = \hat{\theta}_0 + \hat{\theta}_1||\boldsymbol{\xi}|| + \gamma, \tag{19}$$

where $\hat{\theta}_i$ is the estimate of θ_i^*, $i = 0, 1$; γ is an auxiliary gain with a role in closed-loop system stabilization. The gains $\hat{\theta}_i, \gamma$ are evaluated using the following laws:

$$\dot{\hat{\theta}}_i = (||\mathbf{r}|| + ||\boldsymbol{\xi_u}||)||\boldsymbol{\xi}||^i - \eta_i\hat{\theta}_i\beta||\boldsymbol{\xi_u}||||\boldsymbol{\xi}||^i,\ i = 0, 1 \tag{20a}$$

$$\dot{\gamma} = -\gamma\left(\gamma_0 + \gamma_1||\boldsymbol{\xi_u}|| + \gamma_2||\boldsymbol{\xi}||^4\right) + (||\mathbf{r}|| + ||\boldsymbol{\xi_u}||) + \gamma_0\overline{\gamma}, \tag{20b}$$

$$\text{with } \beta > 1 + \overline{\varsigma}\ \text{ where } ||\mathbf{P_uB\Gamma}|| \leq \overline{\varsigma}, \tag{20c}$$

$$\hat{\theta}_i(0) > 0,\ \gamma(0) > \overline{\gamma}, \tag{20d}$$

where $\eta_i, \gamma_0, \gamma_1, \gamma_2, \overline{\gamma} \in \mathbb{R}^+$ are design constants. The gain $\overline{\varsigma}$ can be designed using the known upper bound of the perturbed $\mathbf{M}$ (cf. Assumption 1). The term ρ essentially upper bounds the uncertainties in an adaptive and state-dependent

This article has been accepted for publication in a future issue of this journal, but has not been fully edited. Content may change prior to final publication. Citation information: DOI 10.1109/TMECH.2021.3052068, IEEE/ASME Transactions on Mechatronics

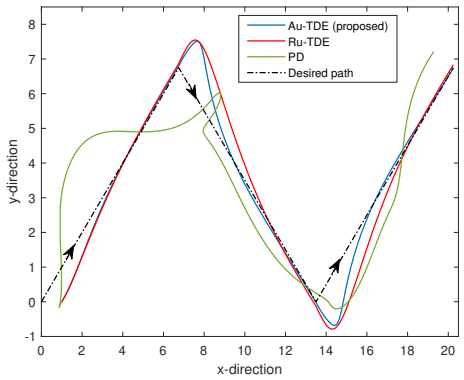

Figure 2. Robotic ship test case, paths for different schemes: proposed adaptive under-actuated TDE, robust under-actuated TDE, linear PD.

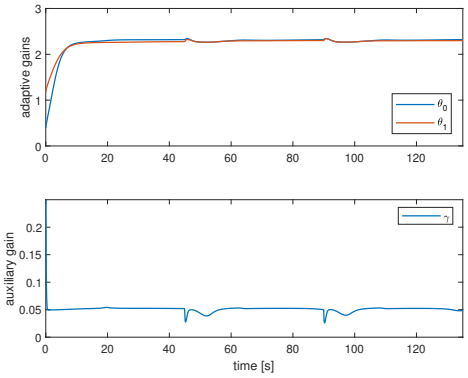

Figure 3. Robotic ship test case: adaptive gains for the proposed adaptive under-actuated TDE (Au-TDE) approach.

way. Differently from standard artificial delay approaches with constant upper bound, a state-dependent upper bound helps shaping the uncertainty according to the state [45].

IV. Stability and Robustness Analysis

A diagram summarizing the proposed controller is shown in Fig. 1. Stability and robustness properties are given below.

Theorem 1. *Under Assumption 1 and Lemma 1, the closed-loop trajectories of (5) with control laws (7), (19) and adaptive law (20) are Uniformly Ultimately Bounded (UUB).*

Proof. See Appendix. □

Remark 4 (Role of γ)**.** *The upper bound of uncertainty $\overline{\phi}_2$ is a quadratic polynomial of $||\boldsymbol{\xi}||$ as in (18), which translates into a third-order term $\theta_2^{**}||\boldsymbol{\xi}||^3$ during stability analysis (cf. first inequality in (49)). This third-order term is tackled by the term $\gamma_2||\boldsymbol{\xi}||^4$ provided by the adaptive law of γ so as to ensure closed-loop stability (cf. the discussion below (49)).*

Remark 5 (Design guidelines)**.** *From (15) it can be noted that the behaviour of the non-actuated dynamics can be tuned via $\mathbf{K_{Pu}}, \mathbf{K_{Du}}$, through (14). High values of η_i, γ_1 and γ_2 lead to high $\underline{\gamma}^2\gamma_2$ and small ι_i, ι_i': this improves the convergence of the polynomials $f(||\boldsymbol{\xi}||)$ and $\overline{f}(||\boldsymbol{\xi}||)$ to $f(||\boldsymbol{\xi}||) < 0$ and $\overline{f}(||\boldsymbol{\xi}||) < 0$ (cf. the negative fifth degree terms in (49) and (53) in the proof). However, such high values might lead to high control input and therefore, these gains should be selected according to application requirements.*

V. Validation

To evaluate the effectiveness of the proposed framework, we consider robotic ship and robotic aerial vehicle test cases.

A. Robotic ship test case

Surface vehicles dynamics are a very common test case for under-actuated robotics [33], and can be written as:

$$\begin{cases} \begin{bmatrix} \dot{x} \\ \dot{\psi} \\ \dot{y} \end{bmatrix} = \begin{bmatrix} \cos\psi & 0 & -\sin\psi \\ 0 & 1 & 0 \\ \sin\psi & 0 & \cos\psi \end{bmatrix} \begin{bmatrix} u \\ r \\ v \end{bmatrix} \\ \begin{bmatrix} m_x & 0 & 0 \\ 0 & I_z & m_{yz} \\ 0 & m_{yz} & m_y \end{bmatrix} \begin{bmatrix} \dot{u} \\ \dot{r} \\ \dot{v} \end{bmatrix} = \\ \qquad \begin{bmatrix} m_y v r + m_{yz} r^2 - d_{11} u \\ -(m_y - m_x) uv - m_{yz} ur - d_{32} v - d_{33} r \\ -m_x ur - d_{22} v - d_{23} r \end{bmatrix} + \begin{bmatrix} \tau_1 \\ \tau_2 \\ 0 \end{bmatrix} \end{cases} \tag{21}$$

where (x, y) denotes the position in Earth-fixed frame; ψ the heading angle with respect to North; u, v, r denote the velocity in surge, sway and yaw, respectively; τ_1 and τ_2 are surge force and sway moment. The actual system parameters are taken from the CyberShip II benchmark by Norwegian University of Science and Technology (NTNU) [28], [29], where m_x, m_y and I are the masses along different axes and the inertia of the ship, and d_{11}, d_{22}, d_{23}, d_{32}, d_{33} are damping terms that take a complex nonlinear form (cf. the details in [28], [29]). Note that the proposed control just needs nominal knowledge of the mass matrix (in line with Lemma 1), whereas centripetal, Coriolis and damping terms can be completely unknown.

The initial configuration of the ship is $(x(0), y(0), \psi(0)) = (2, 0, \pi/4)$ and zero speed. We select the artificial delay $L = 0.1$s, and the various control design parameters are $\mathbf{K_{Pa}} = 5\mathbf{I}, \mathbf{K_{Da}} = 8\mathbf{I}, \mathbf{K_{Du}} = 5[1\ 1]^T, \mathbf{K_{Du}} = 8[1\ 1]^T, \mathbf{Q_a} = 0.001\mathbf{I}$, $\epsilon = 0.1$, $\eta_0 = 1, \eta_1 = 1, \gamma_0 = 1, \gamma_1 = 0.01, \gamma_2 = 0.03, \overline{\gamma} = 0.003$, $\hat{\theta}_0(0) = 0.01, \hat{\theta}_1(0) = 0.1, \gamma(0) = 10$ and $\beta = 3$. For comparison purposes, two other approaches are used. The first approach, named robust under-actuated TDE (Ru-TDE), is an under-actuated TDE version inspired by [7], where the use of a state-dependent bound had been shown to outperform standard TDE approaches [1], [6]; we use constants $\hat{\theta}_0(t) = \hat{\theta}_1(t) = 3.5$, $\forall t$ as upper bound. The second approach is a proportional-derivative (PD) control, which corresponds to removing the artificial delay (7b) and the

This article has been accepted for publication in a future issue of this journal, but has not been fully edited. Content may change prior to final publication. Citation information: DOI 10.1109/TMECH.2021.3052068, IEEE/ASME Transactions on Mechatronics

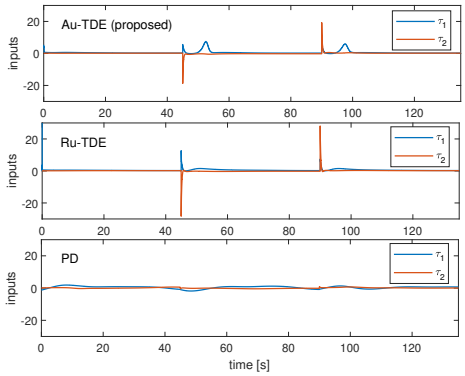

Figure 4. Robotic ship test case, inputs for different schemes: proposed adaptive under-actuated TDE, robust under-actuated TDE, linear PD.

robustifying gain (7c). The proposed adaptive under-actuated TDE approach is abbreviated with Au-TDE.

Fig. 2 shows the tracking of the ship for a complex zigzag maneuver (also known as Z-maneuver or Kempf maneuver), in the presence of sinusoidal disturbances $\mathbf{d_s} = 0.1\cos 0.1t$ in both x and y direction, representing wind/currents. The proposed Au-TDE has the best performance. The effectiveness of the proposed design comes from the adaptive gains: it can be seen from Fig. 3 that $\hat{\theta}_0$ and $\hat{\theta}_1$ converge at around 2.3. On the other hand, the Ru-TDE uses the larger value of 3.5 which leads to larger spikes in the control input (cf. Fig. 4). The linear PD is unable to provide acceptable performance.

B. Robotic aerial vehicle test case

The performance of the proposed controller is tested on a robotic aerial vehicle moving over some walls with a payload: this scenario is important for aerial transport in urban/indoor scenarios [46], [47]. A Gazebo simulation platform using the RotorS Simulator [48] for ROS with the Pelican quadrotor model is adopted. The results of the proposed Au-TDE is compared with an Adaptive Integral Backstepping (AIB) method [38] and with Ru-TDE. A scenario is created in the 'indoor environment' in the RotorS simulator, where the quadrotor is required to perform the following actions sequentially (cf. Fig. 5), while following a minimum snap trajectory:

- From an initial position the quadrotor (unloaded) moves to the first payload location;
- it picks up a payload of 0.3 kg (at approx $t = 32$s) and moves over a wall to the other side and delivers the payload (at approx $t = 58$s);
- then, it moves towards a second payload of 1.0 kg and picks it (at approx $t = 83$s);
- then, it moves over the wall back to the initial position and delivers the payload (at approx $t = 123$s).

The mass of the quadrotor without payload is 4.0 kg. The RotorS simulator exploits the Gazebo physical modelling approach according to the gazebo::physics::Model Class Reference, which means that adding a payload will automatically change the mass and moment of inertia of the entire system. Note that the proposed adaptive control design is not based on mass/inertia estimation. Instead of estimating the mass/inertia and using it to find the appropriate control gains (indirect adaptive control approach [43], [49]), the proposed adaptive laws directly estimate the control gains (direct adaptive control approach). Systems with different mass/inertia will lead to different control estimates. Further, we have added a wind disturbance (random function with normal distribution in Gazebo grids) of mean speed 2 m/s blowing in 45^o direction to x-y plane: this creates a persistent uncertainty term.

The following parameters are selected: $L = 0.01$s, $\mathbf{K_{P}}_a = 5\mathbf{I}, \mathbf{K_{D}}_a = 16\mathbf{I}, \mathbf{K_{P}}_u = 8[1\ 1]^T, \mathbf{K_{D}}_u = 10[1\ 1]^T$, $\mathbf{Q_a} = \mathbf{I}$, $\epsilon = 0.1$, $\eta_0 = 1, \eta_1 = 1, \gamma_0 = 1, \gamma_1 = \gamma_2 = 0.01, \overline{\gamma} = 0.001$, $\hat{\theta}_0(0) = \hat{\theta}_1(0) = 0.01, \gamma(0) = 0.1$ and $\beta = 7$. For Ru-TDE, constant upper bound for $\hat{\theta}_0 = \hat{\theta}_1 = 4$ are used. For AIB, The gains c_1, λ_1 (cf. [38] for the definition) are selected as $c_1 = 8$, $\lambda_1 = 5$ and nominal mass of the system is selected as 4kg. Based upon user-defined desired position trajectories (x^d, y^d, z^d) (cf. Fig. 6) and desired heading angle ψ^d (0 degree here), the desired roll (ϕ^d) and pitch (θ^d) trajectories are generated via the minimum-snapping methods as in [50] (details omitted due to lack of space).

Figures 6-8 show the position responses with various controllers and their corresponding tracking errors. The position responses in Ru-TDE becomes constant for $t > 92$s as the quadrotor topples: though the quadrotor manages to lift the first payload, it could not lift the second payload high enough to cross the wall. This happened because Ru-TDE relies on a priori fixed gains based on predefined uncertainty bounds; when the payload becomes heavier than expected, the controller cannot adjust its gain to adapt to larger uncertainty. On the other hand, AIB requires a priori knowledge of system mass and considers the uncertainties to be bounded a priori by a constant: however, when system mass/inertia is perturbed and under non-constant wind disturbance, such assumptions may be violated. As a result, AIB lost significant tracking performance, especially when the desired trajectories take sharp turns (for example cf. $t = 40, 60, 90, 120$s for z position). On the other hand, the proposed Au-TDE is built upon state-dependent uncertainties (cf. Lemma 1 and (19)) and, thanks to its adaptive gains, it can tackle uncertainties without any a priori knowledge. Table I shows that this strategy outperforms the other controllers in terms of root-mean-squared (RMS) error (the data in the parentheses give performance degradation of the respective controller with respect to Au-TDE).

Table I
PERFORMANCE COMPARISON FOR AERIAL VEHICLE (PERCENTAGES INDICATE DEGRADATION WITH RESPECT TO THE PROPOSED AU-TDE)

Position	RMS error in Position (m)		
	Ru-TDE	AIB	Au-TDE (proposed)
x	3.43 (97.1%)	0.16 (37.3%)	0.10
y	0.98 (90.8%)	0.13 (30.8%)	0.09
z	0.84 (86.9%)	0.27 (59.2%)	0.11
	RMS error in attitude (degree)		
roll (ϕ)	2.53 (45.1%)	1.85 (24.8%)	1.39
pitch (θ)	6.83 (86.8%)	0.92 (2.17%)	0.90
heading (ψ)	0.59 (71.2%)	0.22 (22.7%)	0.17

This article has been accepted for publication in a future issue of this journal, but has not been fully edited. Content may change prior to final publication. Citation information: DOI 10.1109/TMECH.2021.3052068, IEEE/ASME Transactions on Mechatronics

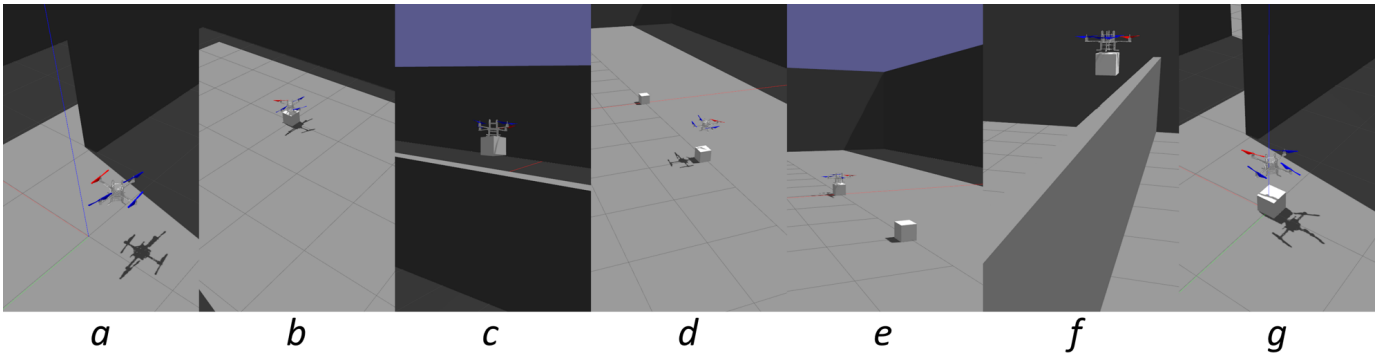

Figure 5. Robotic aerial vehicle test case, snapshots from experimental scenario (with Au-TDE): quadrotor (a) starting from initial position (b) picking up first payload (0.3 kg) (c) moving over a wall with first payload (d) dropping the first payload (e) picking up second payload (1 kg) (f) moving over the wall with second payload (g) dropping the second payload at initial position.

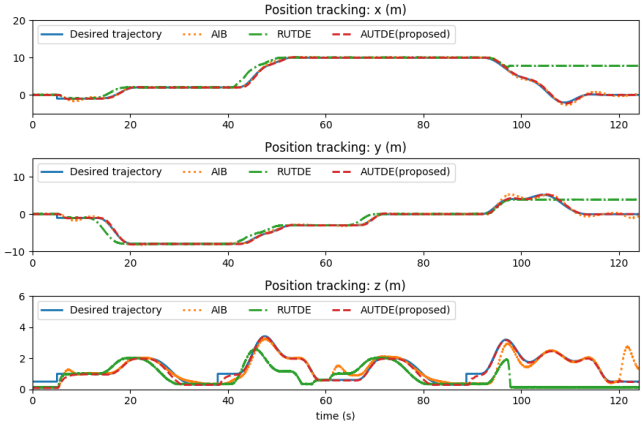

Figure 6. Robotic aerial vehicle test case: position tracking by different controllers (proposed Au-TDE, Ru-TDE, AIB) with variable payloads.

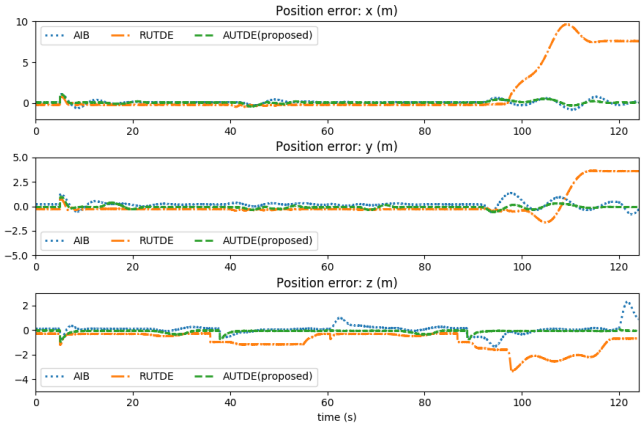

Figure 7. Robotic aerial vehicle test case: position tracking error by different controllers (proposed Au-TDE, Ru-TDE, AIB) with variable payloads.

VI. Experimental Results

In this section, we provide experimental results using a quadrotor to verify the effectiveness of the proposed Au-TDE compared to Ru-TDE and AIB [38] methods. The experimental scenario consists of the following actions to be sequentially performed by the quadrotor (cf. Fig. 9)

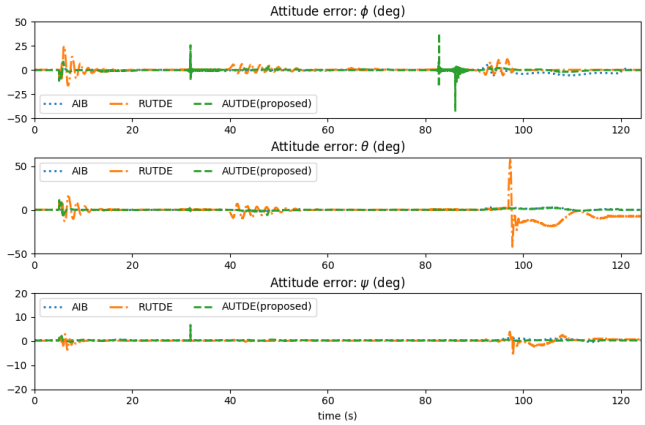

Figure 8. Robotic aerial vehicle test case: attitude (roll (ϕ), pitch (θ), heading (ψ)) tracking error by different controllers (proposed Au-TDE, Ru-TDE, AIB) with variable payloads.

- From an initial position (and without any payload) the quadrotor first ascends, then moves horizontally to the payload location;
- The quadrotor descends to pick up a payload of 0.3 kg (approx.) at around $t = 32$s;
- The quadrotor moves towards a second location to drop the payload.

The quadrotor setup includes 1 bluefox camera, 1 inertial measurement unit, 1 gripper (0.2 kg approx.) and 1 Intel NUC processing unit. Without any payload and excluding sensor suits, the quadrotor weighs 4 kg (approx.). We have used AprilTags at predefined locations, which the camera uses to determine quadrotor location. Via such visual feedback (50 fps) and inertial measurement unit data, all the necessary feedbacks are obtained for control design. It is to be mentioned that the gripper operations, i.e., to open, grip and release payload are not part of the control design and they are operated via a remote signal.

The following parameters are selected $\mathbf{K_{P}}_a = 8\mathbf{I}, \mathbf{K_{D}}_a = 20\mathbf{I}, \mathbf{K_{P}}_u = 7[1\ 1]^T, \mathbf{K_{D}}_u = 12[1\ 1]^T, \mathbf{Q_a} = \mathbf{I}$, $\epsilon = 0.1$, $\eta_0 = 1, \eta_1 = 1, \gamma_0 = 1, \gamma_1 = \gamma_2 = 0.01, \overline{\gamma} = 0.001$, $\hat{\theta}_0(0) = \hat{\theta}_1(0) = 0.01, \gamma(0) = 0.1$ and $\beta = 8$. For Ru-TDE, constant upper bound for $\hat{\theta}_0 = \hat{\theta}_1 = 3$ are used. Considering

This article has been accepted for publication in a future issue of this journal, but has not been fully edited. Content may change prior to final publication. Citation information: DOI 10.1109/TMECH.2021.3052068, IEEE/ASME Transactions on Mechatronics

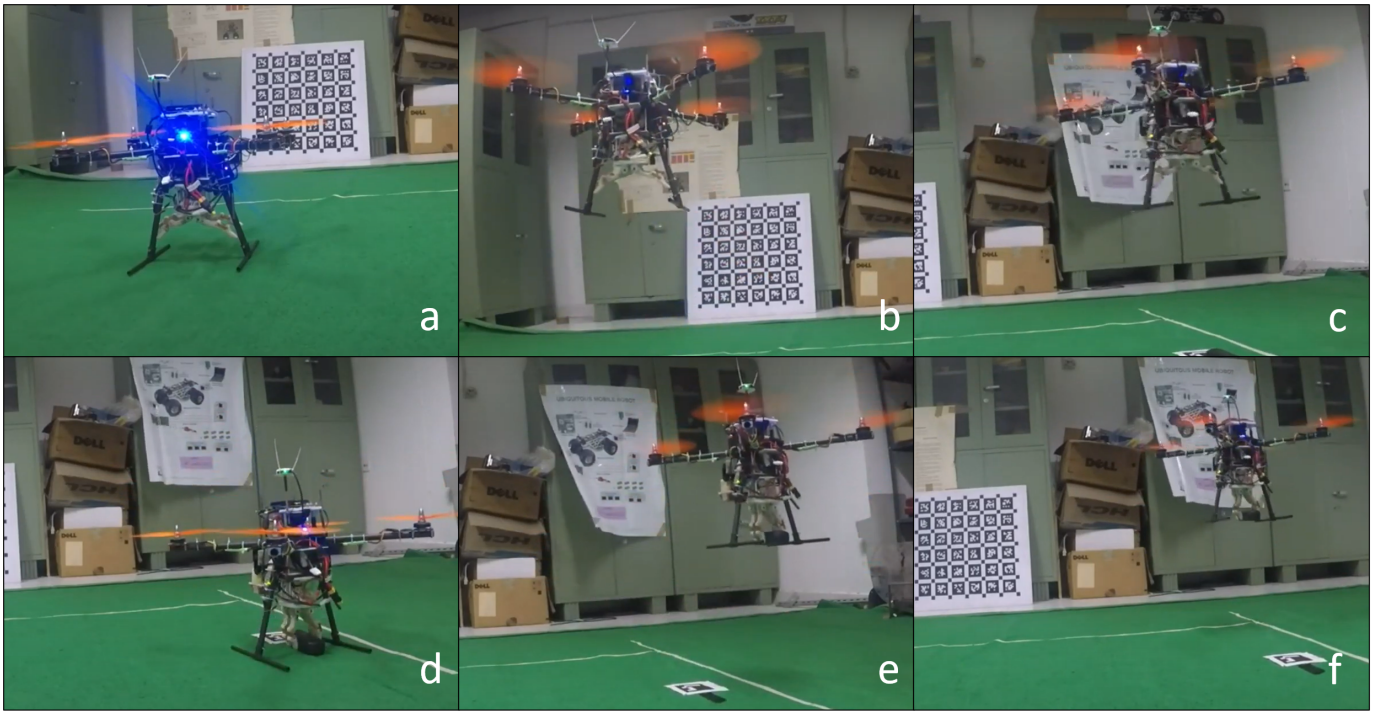

Figure 9. Snapshots from experimental scenario (with Au-TDE): quadrotor (a) starting from initial position (b) moving toward the payload (c) descending to pick up payload (d) picking up the payload (0.3 kg) (e) moving with the payload (f) dropping the payload at final position.

the processing time for visual feedback, $L = 0.02$s is selected for both Ru-TDE and Au-TDE. For AIB, the gains are selected as $c_1 = 10$, $\lambda_1 = 5$ and mass of the system is selected as 4kg.

The tracking performance of various controllers are depicted via Figs. 10-12 and Table II. The error plots depict that the performance of all the controllers are close before the payload is attached at $t \approx 32$s. However, after the quadrotor ascends with the payload, different performances become evident: with the help of its integral control, AIB has better tracking error than Ru-TDE, but it significantly falls behind the proposed Au-TDE. As mentioned earlier, this is because variation in system mass creates state-dependent uncertainty which AIB is not designed to handle. Owing to the capabilities to handle unknown and non a priori bounded state-dependent uncertainties and external disturbances, Au-TDE is able to outperform other methods (cf. Table II).

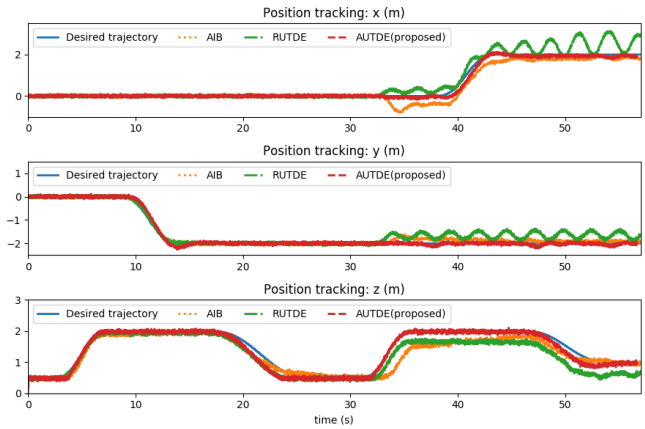

Figure 10. Position tracking by different controllers during experiment.

Table II
PERFORMANCE COMPARISON DURING EXPERIMENT WITH QUADROTOR (PERCENTAGES INDICATE DEGRADATION WITH RESPECT TO THE PROPOSED AU-TDE)

Position	RMS error in Position (m)		
	Ru-TDE	AIB	Au-TDE (proposed)
x	0.51 (78.4%)	0.26 (53.8%)	0.11
y	0.34 (70.5%)	0.13 (23.1%)	0.10
z	0.29 (51.7%)	0.25 (56.0%)	0.13
	RMS error in attitude (degree)		
roll (ϕ)	5.11 (70.4%)	1.61 (6.2%)	1.51
pitch (θ)	7.52 (83.9%)	3.42 (64.6%)	1.21
heading (ψ)	0.73 (65.7%)	0.42 (40.4%)	0.25

Interesting future works would be to demonstrate the proposed approach in more challenging scenarios such as aggressive maneuvers with payloads [51] and with slung payloads [52], [53]. These are beyond the scope of this work as it requires a sophisticated motion capture system and advanced Kalman filtering techniques not covered in this work.

VII. CONCLUSIONS AND FUTURE WORK

Artificial-delay control is a simple control methodology with various robotic applications where uncertain system dynamics are compensated using past input and state measurements. In contrast with the state-of-the-art that has proven stability and robustness of artificial-delay control for fully-

This article has been accepted for publication in a future issue of this journal, but has not been fully edited. Content may change prior to final publication. Citation information: DOI 10.1109/TMECH.2021.3052068, IEEE/ASME Transactions on Mechatronics

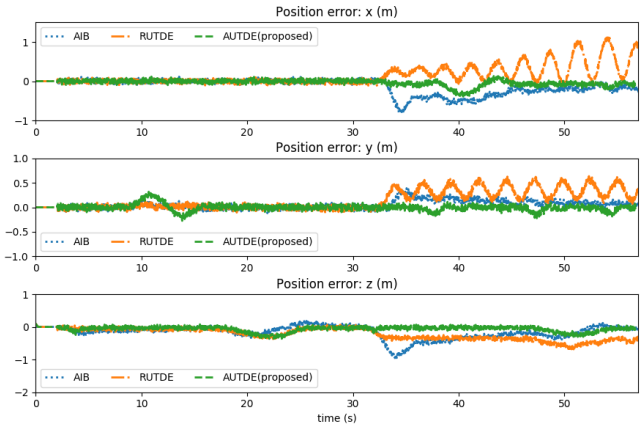

Figure 11. Position tracking error by different controllers for experiment.

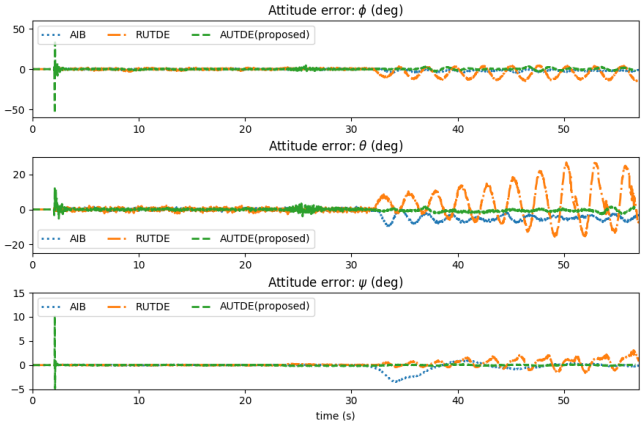

Figure 12. Attitude tracking error by different controllers for experiment with quadrotor: roll (ϕ), pitch (θ), heading (ψ).

actuated systems, in this work we have proposed an artificial-delay control scheme in the presence of under-actuation. We expect the proposed solution to find application in all those fields where artificial delay has been successfully applied, since the presented framework inherits the same time delay estimation (TDE) philosophy. The standard TDE approach uses a constant upper bound for uncertainty, whereas the TDE mechanism we used a state-dependent bound requiring an extra estimator. There are at least three long-standing open problems in artificial delay literature that are worth of future consideration: the design of an artificial delay control free of acceleration feedback; the design of an artificial delay control explicitly taking non-ideal actuation into account (delay, saturation); the design of high-order artificial-delay methods, in line with high-order sliding mode methods [54].

APPENDIX

PROOF OF LEMMA 1

From (6) and (7), the following relations can be achieved:

$$\hat{\overline{\mathbf{h}}}_{\mathbf{a}} = (\overline{\mathbf{h}}_{\mathbf{a}})_L = [(\mathbf{M_s})_L - \overline{\mathbf{M}}_{\mathbf{a}}](\ddot{\mathbf{q}}_{\mathbf{a}})_L - (\mathbf{h_a})_L, \tag{22}$$

$$\boldsymbol{\sigma}_{\mathbf{a}} = \ddot{\mathbf{q}}_{\mathbf{a}} - \boldsymbol{\nu}. \tag{23}$$

Using (22), the control input $\boldsymbol{\tau}$ in (7a) can be rewritten as

$$\boldsymbol{\tau} = \overline{\mathbf{M}}_{\mathbf{a}}\boldsymbol{\nu} + [(\mathbf{M_s})_L - \overline{\mathbf{M}}_{\mathbf{a}}](\ddot{\mathbf{q}}_{\mathbf{a}})_L - (\mathbf{h_a})_L. \tag{24}$$

Multiplying both sides of (23) with $\mathbf{M_s}$ and using (5b) and (24) we arrive at

$$\begin{aligned}\mathbf{M_s}\boldsymbol{\sigma}_{\mathbf{a}} = \overline{\mathbf{M}}_{\mathbf{a}}\boldsymbol{\nu} + [(\mathbf{M_s})_L - \overline{\mathbf{M}}_{\mathbf{a}}](\ddot{\mathbf{q}}_{\mathbf{a}})_L \\ - (\mathbf{h_a})_L + \mathbf{h_a} - \mathbf{M_s}\boldsymbol{\nu}.\end{aligned} \tag{25}$$

Defining $\mathbf{K} \triangleq [\mathbf{K_{Pa}}\ \mathbf{K_{Pu}}\ \mathbf{K_{Da}}\ \mathbf{K_{Du}}]$ and using (8) we have

$$(\ddot{\mathbf{q}}_{\mathbf{a}})_L = (\ddot{\mathbf{q}}^d_{\mathbf{a}})_L - \mathbf{K}\boldsymbol{\xi}_L - (\Delta\boldsymbol{\tau})_L + (\boldsymbol{\sigma}_{\mathbf{a}})_L, \tag{26}$$

Substituting (26) to (25) yields

$$\begin{aligned}\boldsymbol{\sigma}_{\mathbf{a}} = &\underbrace{\mathbf{M_s}^{-1}\overline{\mathbf{M}}_{\mathbf{a}}((\Delta\boldsymbol{\tau})_L - \Delta\boldsymbol{\tau})}_{\boldsymbol{\chi}_1} + \underbrace{\mathbf{M_s}^{-1}(\mathbf{M_s}\Delta\boldsymbol{\tau} - (\mathbf{M_s})_L(\Delta\boldsymbol{\tau})_L)}_{\boldsymbol{\chi}_2} \\ &+ \underbrace{\mathbf{M_s}^{-1}\{(\overline{\mathbf{M}}_{\mathbf{a}} - \mathbf{M_s})\ddot{\mathbf{q}}^d_{\mathbf{a}} - (\overline{\mathbf{M}}_{\mathbf{a}} - (\mathbf{M_s})_L)(\ddot{\mathbf{q}}^d_{\mathbf{a}})_L + \mathbf{h_a} - (\mathbf{h_a})_L\}}_{\boldsymbol{\chi}_3} \\ &+ \underbrace{\mathbf{M_s}^{-1}(\overline{\mathbf{M}}_{\mathbf{a}} - (\mathbf{M_s})_L)\mathbf{K}\boldsymbol{\xi}_L}_{\boldsymbol{\chi}_4} - \underbrace{\mathbf{M_s}^{-1}(\overline{\mathbf{M}_{\mathbf{a}}} - (\mathbf{M_s})_L)(\boldsymbol{\sigma}_{\mathbf{a}})_L}_{\boldsymbol{\chi}_5} \\ &+ \underbrace{(\mathbf{I} - \mathbf{M_s}^{-1}\overline{\mathbf{M}}_{\mathbf{a}})\mathbf{K}\boldsymbol{\xi}}_{\boldsymbol{\chi}_6}.\end{aligned} \tag{27}$$

The system property (2) implies $\mathbf{M_s}$ and $\mathbf{M_s}^{-1}$ are bounded. Any function ψ delayed as $\psi(t-L) = \psi_L$ can be written as

$$\psi_L = \psi(t-L) = \psi(t) - \int_{-L}^{0} \frac{\mathrm{d}}{\mathrm{d}\theta}\psi(t+\theta)\,\mathrm{d}\theta. \tag{28}$$

Integration of any bounded function over a finite interval is always finite. Therefore, using (28) and the interval from $-L$ to 0, the following conditions hold for unknown constants $\delta_i, i = 1, \cdots, 5$:

$$||\boldsymbol{\chi}_1|| = ||-\mathbf{M_s}^{-1}\overline{\mathbf{M}}_{\mathbf{a}}\int_{-L}^{0}\frac{\mathrm{d}}{\mathrm{d}\theta}\Delta\boldsymbol{\tau}(t+\theta)\,\mathrm{d}\theta|| \le \delta_1 \tag{29}$$

$$||\boldsymbol{\chi}_2|| = ||\mathbf{M_s}^{-1}\int_{-L}^{0}\frac{\mathrm{d}}{\mathrm{d}\theta}\mathbf{M_s}(t+\theta)\Delta\boldsymbol{\tau}(t+\theta)\,\mathrm{d}\theta|| \le \delta_2 \tag{30}$$

$$\begin{aligned}||\boldsymbol{\chi}_3|| = ||\mathbf{M_s}^{-1}\int_{-L}^{0}\frac{\mathrm{d}}{\mathrm{d}\theta}\{(\overline{\mathbf{M}}_{\mathbf{a}} - \mathbf{M_s}(t+\theta))\ddot{\mathbf{q}}^d_{\mathbf{a}}(t+\theta) \\ + \mathbf{h_a}(t+\theta)\}\,\mathrm{d}\theta|| \le \delta_3\end{aligned} \tag{31}$$

$$\begin{aligned}||\boldsymbol{\chi}_4|| = ||(\mathbf{M_s}^{-1}\overline{\mathbf{M}}_{\mathbf{a}} - \mathbf{I})\mathbf{K}\boldsymbol{\xi} \\ + \mathbf{M_s}^{-1}\int_{-L}^{0}\frac{\mathrm{d}}{\mathrm{d}\theta}(\mathbf{M_s}(t+\theta) - \overline{\mathbf{M}}_{\mathbf{a}})\mathbf{K}\boldsymbol{\xi}(t+\theta)\,\mathrm{d}\theta|| \\ \le ||\mathbf{EK}||||\boldsymbol{\xi}|| + \delta_4\end{aligned} \tag{32}$$

$$\begin{aligned}||\boldsymbol{\chi}_5|| = ||\mathbf{E}\boldsymbol{\sigma}_{\mathbf{a}} + \mathbf{M_s}^{-1}\int_{-L}^{0}\frac{\mathrm{d}}{\mathrm{d}\theta}(\mathbf{M_s}(t+\theta) - \overline{\mathbf{M}}_{\mathbf{a}})\boldsymbol{\sigma}_{\mathbf{a}}(t+\theta)\,\mathrm{d}\theta|| \\ \le ||\mathbf{E}||||\boldsymbol{\sigma}_{\mathbf{a}}|| + \delta_5\end{aligned} \tag{33}$$

$$||\boldsymbol{\chi}_6|| = ||(\mathbf{M_s}^{-1}\overline{\mathbf{M}}_{\mathbf{a}} - \mathbf{I})\mathbf{K}\boldsymbol{\xi}|| \le ||\mathbf{EK}||||\boldsymbol{\xi}||. \tag{34}$$

Define $||\mathbf{E}|| = ||\mathbf{I} - \mathbf{M_s}^{-1}\overline{\mathbf{M}}_{\mathbf{a}}||$. Then, if $\overline{\mathbf{M}}_{\mathbf{a}}$ is selected such that (10) holds, the upper bound of $\boldsymbol{\sigma}_{\mathbf{a}}$ is formulated using (29)-(34) from (27) as (9), with

$$\theta_0 = \frac{1}{1-||\mathbf{E}||}\sum_{i=1}^{5}\delta_i,\ \theta_1 = \frac{2||\mathbf{EK}||}{1-||\mathbf{E}||}. \tag{35}$$

PROOF OF THEOREM 1

Stability is analyzed using the following Lyapunov function:

$$V = \frac{1}{2}\boldsymbol{\xi}_{\mathbf{a}}^T\mathbf{P}_{\mathbf{a}}\boldsymbol{\xi}_{\mathbf{a}} + \frac{1}{2}\boldsymbol{\xi}_{\mathbf{u}}^T\mathbf{P}_{\mathbf{u}}\boldsymbol{\xi}_{\mathbf{u}} + \sum_{i=0}^{1}\frac{(\hat{\theta}_i - \overline{\theta}_i)^2}{2} + \frac{\gamma^2}{2}, \quad (36)$$

where $\overline{\theta}_i = \max\{\theta_i^*, \theta_i^{**}\}$. We shall proceed the stability analysis for the two cases (i) $||\mathbf{r}|| \geq \epsilon$ and (ii) $||\mathbf{r}|| < \epsilon$ using the common Lyapunov function (36).

Case (i) $||\mathbf{r}|| \geq \epsilon$

Using (7c), (8), (11) and (19), we have

$$\begin{aligned}\frac{1}{2}\frac{\mathrm{d}}{\mathrm{d}t}\boldsymbol{\xi}_{\mathbf{a}}^T\mathbf{P}_{\mathbf{a}}\boldsymbol{\xi}_{\mathbf{a}} &\leq -\frac{1}{2}\boldsymbol{\xi}_{\mathbf{a}}^T\mathbf{Q}_{\mathbf{a}}\boldsymbol{\xi}_{\mathbf{a}} - \rho||\mathbf{r}|| + ||\boldsymbol{\phi}_1||||\mathbf{r}|| \\ &\leq -\frac{1}{2}\boldsymbol{\xi}_{\mathbf{a}}^T\mathbf{Q}_{\mathbf{a}}\boldsymbol{\xi}_{\mathbf{a}} - \sum_{i=0}^{1}\hat{\theta}_i||\boldsymbol{\xi}||^i||\mathbf{r}|| + \sum_{i=0}^{1}\overline{\theta}_i||\boldsymbol{\xi}||^i||\mathbf{r}||. \quad (37)\end{aligned}$$

Further, using (16) and (18)

$$\begin{aligned}\frac{1}{2}\frac{\mathrm{d}}{\mathrm{d}t}\boldsymbol{\xi}_{\mathbf{u}}^T\mathbf{P}_{\mathbf{u}}\boldsymbol{\xi}_{\mathbf{u}} &\leq -\frac{1}{2}\boldsymbol{\xi}_{\mathbf{u}}^T\mathbf{Q}_{\mathbf{u}}\boldsymbol{\xi}_{\mathbf{u}} + \rho\overline{\varsigma}||\mathbf{x}|| + ||\overline{\boldsymbol{\phi}}_2||||\mathbf{PB}||||\boldsymbol{\xi}_{\mathbf{u}}|| \\ &\leq -\frac{1}{2}\boldsymbol{\xi}_{\mathbf{u}}^T\mathbf{Q}_{\mathbf{u}}\boldsymbol{\xi}_{\mathbf{u}} + \overline{\varsigma}\sum_{i=0}^{1}(\hat{\theta}_i||\boldsymbol{\xi}||^i + \gamma)||\boldsymbol{\xi}_{\mathbf{u}}|| \\ &\quad + \sum_{i=0}^{1}\overline{\theta}_i||\boldsymbol{\xi}||^i||\boldsymbol{\xi}_{\mathbf{u}}|| + \theta_2^{**}||\boldsymbol{\xi}||^2||\boldsymbol{\xi}_{\mathbf{u}}||. \quad (38)\end{aligned}$$

Using the adaptive laws (20a) and (20b), we have, for $i = 0, 1$

$$\begin{aligned}(\hat{\theta}_i - \overline{\theta}_i)\dot{\hat{\theta}}_i &= \hat{\theta}_i(||\mathbf{r}|| + ||\boldsymbol{\xi}_{\mathbf{u}}||)||\boldsymbol{\xi}||^i - c_i\hat{\theta}_i^2||\boldsymbol{\xi}_{\mathbf{u}}||||\boldsymbol{\xi}||^i \\ &\quad - \overline{\theta}_i(||\mathbf{r}|| + ||\boldsymbol{\xi}_{\mathbf{u}}||)||\boldsymbol{\xi}||^i + c_i\hat{\theta}_i\overline{\theta}_i||\boldsymbol{\xi}_{\mathbf{u}}||||\boldsymbol{\xi}||^i, \quad (39) \\ \gamma\dot{\gamma} &= \gamma(||\mathbf{r}|| + ||\boldsymbol{\xi}_{\mathbf{u}}||) \\ &\quad - \gamma^2(\gamma_0 + \gamma_1||\boldsymbol{\xi}_{\mathbf{u}}|| + \gamma_2||\boldsymbol{\xi}||^4) + \gamma\gamma_0\overline{\gamma}, \quad (40)\end{aligned}$$

with $c_i \triangleq \eta_i\beta$ a positive scalar (cf. (20a) and (20c)). Therefore,

$$\begin{aligned}&\frac{\mathrm{d}}{\mathrm{d}t}\left(\sum_{i=0}^{1}\frac{(\hat{\theta}_i - \overline{\theta}_i)^2}{2} + \frac{\gamma^2}{2}\right) = \sum_{i=0}^{1}\hat{\theta}_i(||\mathbf{r}|| + ||\boldsymbol{\xi}_{\mathbf{u}}||)||\boldsymbol{\xi}||^i \\ &- c_i\hat{\theta}_i^2||\boldsymbol{\xi}_{\mathbf{u}}||||\boldsymbol{\xi}||^i - \overline{\theta}_i(||\mathbf{r}|| + ||\boldsymbol{\xi}_{\mathbf{u}}||)||\boldsymbol{\xi}||^i + c_i\hat{\theta}_i\overline{\theta}_i||\boldsymbol{\xi}_{\mathbf{u}}||||\boldsymbol{\xi}||^i \\ &+ \gamma(||\mathbf{r}|| + ||\boldsymbol{\xi}_{\mathbf{u}}||) - \gamma^2(\gamma_0 + \gamma_1||\boldsymbol{\xi}_{\mathbf{u}}|| + \gamma_2||\boldsymbol{\xi}||^4) + \gamma\gamma_0\overline{\gamma}. \quad (41)\end{aligned}$$

Using (37), (38) and (41), the time derivative of (36) becomes

$$\begin{aligned}\dot{V} &\leq -\delta_m(||\boldsymbol{\xi}_{\mathbf{a}}||^2 + ||\boldsymbol{\xi}_{\mathbf{u}}||^2) + \theta_2^{**}||\boldsymbol{\xi}||^2||\boldsymbol{\xi}_{\mathbf{u}}|| \\ &\quad + \sum_{i=0}^{1}(c\hat{\theta}_i - c_i\hat{\theta}_i^2 + c_i\hat{\theta}_i\overline{\theta}_i)||\boldsymbol{\xi}||^i||\boldsymbol{\xi}_{\mathbf{u}}|| \\ &\quad - \gamma^2(\gamma_0 + \gamma_1||\boldsymbol{\xi}_{\mathbf{u}}|| + \gamma_2||\boldsymbol{\xi}||^4) + \gamma\gamma_0\overline{\gamma} + c\gamma||\boldsymbol{\xi}_{\mathbf{u}}||, \quad (42)\end{aligned}$$

where $\delta_m \triangleq \frac{1}{2}\min\{\lambda_{\min}(\mathbf{Q}_{\mathbf{a}}),\ \lambda_{\min}(\mathbf{Q}_{\mathbf{u}})\}$ and $c \triangleq 1 + \overline{\varsigma}$.

Since $\hat{\theta}_i(t) \geq 0$, the definition of V from (36) yields

$$V \leq \delta_M(||\boldsymbol{\xi}_{\mathbf{a}}||^2 + ||\boldsymbol{\xi}_{\mathbf{u}}||^2) + \sum_{i=0}^{1}(\hat{\theta}_i^2 + \overline{\theta}_i^2) + \gamma^2, \quad (43)$$

where $\delta_M \triangleq \max\{\lambda_{\max}(\mathbf{P}_{\mathbf{a}}),\ \lambda_{\max}(\mathbf{P}_{\mathbf{u}})\}$. Then, defining $\Omega \triangleq (\delta_m/\delta_M)$ and using (43), (42) is simplified to

$$\begin{aligned}\dot{V} &\leq -\Omega V + \sum_{i=0}^{1}\Omega(\hat{\theta}_i^2 + \overline{\theta}_i^2) + \Omega\gamma^2 + \theta_2^{**}||\boldsymbol{\xi}||^2||\boldsymbol{\xi}_{\mathbf{u}}|| \\ &\quad + \sum_{i=0}^{1}(c\hat{\theta}_i - c_i\hat{\theta}_i^2 + c_i\hat{\theta}_i\overline{\theta}_i)||\boldsymbol{\xi}||^i||\boldsymbol{\xi}_{\mathbf{u}}|| + c\gamma||\boldsymbol{\xi}_{\mathbf{u}}|| \\ &\quad - \gamma^2(\gamma_0 + \gamma_1||\boldsymbol{\xi}_{\mathbf{u}}|| + \gamma_2||\boldsymbol{\xi}||^4) + \gamma\gamma_0\overline{\gamma}. \quad (44)\end{aligned}$$

Since c_i and γ_1 are positive constants by design, it is always possible to split these terms in the following way

$$c_i = \sum_{j=1}^{3}c_{ij},\ \gamma_1 = \sum_{k=1}^{2}\gamma_{1k}, \quad c_{ij}, \gamma_{1k} > 0\ \forall i, j, k. \quad (45)$$

The following simplifications can be made:

$$\begin{aligned}&-c_i\hat{\theta}_i^2 + c\hat{\theta}_i + c_i\hat{\theta}_i\overline{\theta}_i \\ &= -c_{i1}\hat{\theta}_i^2 - c_{i2}\left\{\left(\hat{\theta}_i - (c/(2c_{i2}))\right)^2 - (c^2/(4c_{i2}^2))\right\} \\ &\quad - c_{i3}\left\{\left(\hat{\theta}_i - \left((c_i\overline{\theta}_i)/(2c_{i3})\right)\right)^2 - \left((c_i\overline{\theta}_i)^2/(4c_{i3}^2)\right)\right\} \\ &\leq -c_{i1}\hat{\theta}_i^2 + c^2/(4c_{i2}) + (c_i\overline{\theta}_i)^2/(4c_{i3}). \quad (46)\end{aligned}$$

Further,

$$\begin{aligned}&-\gamma^2(\gamma_0 + \gamma_1||\boldsymbol{\xi}_{\mathbf{u}}||) + \gamma\gamma_0\overline{\gamma} + c\gamma||\boldsymbol{\xi}_{\mathbf{u}}|| \\ &= -\gamma_{11}\gamma^2||\boldsymbol{\xi}_{\mathbf{u}}|| - \gamma_0\left\{(\gamma - (\overline{\gamma}/2))^2 - (\overline{\gamma}/2)^2\right\} \\ &\quad - \gamma_{12}||\boldsymbol{\xi}_{\mathbf{u}}||\left\{(\gamma - (c/2\gamma_{12}))^2 - \left(c^2/4\gamma_{12}^2\right)\right\} \\ &\leq -\gamma_{11}\gamma^2||\boldsymbol{\xi}_{\mathbf{u}}|| + \left(c^2/4\gamma_{12}\right)||\boldsymbol{\xi}_{\mathbf{u}}|| + (\overline{\gamma}^2/4). \quad (47)\end{aligned}$$

Investigating the adaptive laws (20a)-(20b) and conditions (20d), it can be verified there exists a positive $\underline{\gamma}$ such that

$$\hat{\theta}_i(t) \geq 0 \text{ and } \gamma(t) \geq \underline{\gamma} > 0 \quad \forall t \geq 0. \quad (48)$$

Since $\gamma \geq \underline{\gamma}$ and $||\boldsymbol{\xi}|| \geq ||\boldsymbol{\xi}_{\mathbf{u}}||$, using (46)-(47), (44) becomes

$$\begin{aligned}\dot{V} &\leq -\Omega V + \sum_{i=0}^{1}\Omega(\hat{\theta}_i^2 + \overline{\theta}_i^2) + \Omega\gamma^2 + (\overline{\gamma}^2/4) + \theta_2^{**}||\boldsymbol{\xi}||^3 \\ &\quad + \sum_{i=0}^{1}\left(\frac{c^2}{4c_{i2}} + \frac{\left(c_i\overline{\theta}_i\right)^2}{4c_{i3}}\right)||\boldsymbol{\xi}||^{i+1} - c_{i1}\hat{\theta}_i^2||\boldsymbol{\xi}_{\mathbf{u}}||^{i+1} \\ &\quad - \underline{\gamma}^2\gamma_2(||\boldsymbol{\xi}||^5 - ||\boldsymbol{\xi}||^4) - \gamma_{11}\gamma^2||\boldsymbol{\xi}_{\mathbf{u}}|| + \left(c^2/4\gamma_{12}\right)||\boldsymbol{\xi}_{\mathbf{u}}|| \\ &= -\Omega V - \hat{\theta}_0^2\left(c_{01}||\boldsymbol{\xi}_{\mathbf{u}}|| - \Omega\right) - \hat{\theta}_1^2\left(c_{11}||\boldsymbol{\xi}_{\mathbf{u}}||^2 - \Omega\right) \\ &\quad - \gamma^2\left(\gamma_{11}||\boldsymbol{\xi}_{\mathbf{u}}|| - \Omega\right) + f(||\boldsymbol{\xi}||), \quad (49)\end{aligned}$$

where $f(||\boldsymbol{\xi}||) \triangleq -\underline{\gamma}^2\gamma_2||\boldsymbol{\xi}||^4 + \omega_3||\boldsymbol{\xi}||^3 + \omega_2||\boldsymbol{\xi}||^2 + \omega_1||\boldsymbol{\xi}|| + \omega_0$,

$$\omega_0 \triangleq \sum_{i=0}^{1}\Omega\overline{\theta}_i^2 + (\overline{\gamma}^2/4),\ \omega_1 \triangleq \frac{c^2}{4c_{02}} + \frac{\left(c_0\overline{\theta}_0\right)^2}{4c_{03}} + \frac{c^2}{4\gamma_{12}},$$

$$\omega_2 \triangleq \frac{c^2}{4c_{12}} + \frac{\left(c_1\overline{\theta}_1\right)^2}{4c_{13}},\ \omega_3 \triangleq \theta_2^{**}.$$

Using Descartes' rule of sign change and Bolzano's Theorem, it can be verified that the polynomial $f(||\boldsymbol{\xi}||)$ has exactly

one positive real root. Let $\iota \in \mathbb{R}^+$ be the positive real root of $f(||\boldsymbol{\xi}||)$. The leading coefficient of $f(||\boldsymbol{\xi}||)$ is negative as $\underline{\gamma}^2\gamma_2 \in \mathbb{R}^+$. Therefore, $f(||\boldsymbol{\xi}||) \leq 0$ when $||\boldsymbol{\xi}|| \geq \iota$. Define $\iota_0 \triangleq \frac{\Omega}{c_{01}}, \iota_1 \triangleq \sqrt{\frac{\Omega}{c_{11}}}$, $\iota_2 \triangleq \frac{\Omega}{\gamma_{11}}$. From (49), $\dot{V} \leq -\Omega V$ when

$$||\boldsymbol{\xi}_\mathbf{u}|| \geq \max\{\iota,\ \iota_0,\ \iota_1,\ \iota_2\}. \tag{50}$$

Case (ii) $||\mathbf{r}|| < \epsilon$

Using (7c), (8), (11) and (19), we have for $||\mathbf{r}|| < \epsilon$

$$\begin{aligned}\frac{1}{2}\frac{\mathrm{d}}{\mathrm{d}t}\boldsymbol{\xi}_\mathbf{a}^T\mathbf{P}_\mathbf{a}\boldsymbol{\xi}_\mathbf{a} &\leq -\frac{1}{2}\boldsymbol{\xi}_\mathbf{a}^T\mathbf{Q}_\mathbf{a}\boldsymbol{\xi}_\mathbf{a} - \rho(||\mathbf{r}||^2/\epsilon) + ||\boldsymbol{\phi}_1||||\mathbf{r}|| \\ &\leq -\frac{1}{2}\boldsymbol{\xi}_\mathbf{a}^T\mathbf{Q}_\mathbf{a}\boldsymbol{\xi}_\mathbf{a} + \sum_{i=0}^{1}\overline{\theta}_i||\boldsymbol{\xi}||^i||\mathbf{r}||. \end{aligned}\tag{51}$$

The following simplification is made for $i = 0, 1$:

$$\begin{aligned}\epsilon\hat{\theta}_i||\boldsymbol{\xi}||^i &= \hat{\theta}_i^2 - \left\{\left(\hat{\theta}_i - (\epsilon||\boldsymbol{\xi}||^i)/2\right)^2 - (\epsilon^2||\boldsymbol{\xi}||^{(2i)})/4\right\} \\ &\leq \hat{\theta}_i^2 + (\epsilon^2||\boldsymbol{\xi}||^{(2i)})/4. \end{aligned}\tag{52}$$

Using (51)-(52) and a similar procedure as Case (i), the following can be deduced for Case (ii):

$$\begin{aligned}\dot{V} \leq &-\Omega V - \hat{\theta}_0^2\left(c_{01}||\boldsymbol{\xi}_\mathbf{u}|| - (\Omega+1)\right) \\ &- \hat{\theta}_1^2\left(c_{11}||\boldsymbol{\xi}_\mathbf{u}||^2 - (\Omega+1)\right) \\ &- \gamma^2\left(\gamma_{11}||\boldsymbol{\xi}_\mathbf{u}|| - (\Omega+1)\right) + \overline{f}(||\boldsymbol{\xi}||), \end{aligned}\tag{53}$$

where $\overline{f}(||\boldsymbol{\xi}||) \triangleq -\underline{\gamma}^2\gamma_2||\boldsymbol{\xi}||^4 + \omega_3||\boldsymbol{\xi}||^3 + \omega_2'||\boldsymbol{\xi}||^2 + \omega_1||\boldsymbol{\xi}|| + \omega_0'$,

$$\omega_2' \triangleq \omega_2 + (\epsilon^2/4),\ \omega_0' \triangleq \sum_{i=0}^{1}\Omega\overline{\theta}_i^2 + \frac{\{\overline{\gamma} + (\epsilon/\gamma_0)\}^2}{4} + \frac{\epsilon^2}{4}.$$

Asserting similar argument made for Case (i), $\dot{V} \leq -\Omega V$ is guaranteed when

$$||\boldsymbol{\xi}_\mathbf{u}|| \geq \max\{\iota',\ \iota_0',\ \iota_1',\ \iota_2'\}, \tag{54}$$

where ι' is the sole positive real root of the polynomial $\overline{f}$ and $\iota_0' \triangleq \left(\frac{\Omega+1}{c_{01}}\right)$, $\iota_1' \triangleq \sqrt{\frac{\Omega+1}{c_{11}}}$ and $\iota_2' \triangleq \left(\frac{\Omega+1}{\gamma_{11}}\right)$. Hence, investigating the stability results for Cases (i) and (ii), it can be concluded that the closed-loop system remains UUB and $\mathbf{e_a}, \dot{\mathbf{e}}_\mathbf{a}, \mathbf{e_u}, \dot{\mathbf{e}}_\mathbf{u}, \hat{\theta}_i, \gamma$ are bounded.

REFERENCES

[1] T. C. S. Hsia, T. A. Lasky, and Z. Guo, "Robust independent joint controller design for industrial robot manipulators," *IEEE Transactions on Industrial Electronics*, vol. 38, no. 1, pp. 21–25, Feb 1991.

[2] T. C. Hsia and L. S. Gao, "Robot manipulator control using decentralized linear time-invariant time-delayed joint controllers," in *Proceedings., IEEE International Conference on Robotics and Automation*, May 1990, pp. 2070–2075 vol.3.

[3] K. Youcef-Toumi and O. Ito, "A Time Delay Controller for Systems With Unknown Dynamics," *Journal of Dynamic Systems, Measurement, and Control*, vol. 112, no. 1, pp. 133–142, 03 1990.

[4] E. Fridman and L. Shaikhet, "Stabilization by using artificial delays: An lmi approach," *Automatica*, vol. 81, pp. 429 – 437, 2017.

[5] A. Selivanov and E. Fridman, "Sampled-data implementation of derivative-dependent control using artificial delays," *IEEE Transactions on Automatic Control*, vol. 63, no. 10, pp. 3594–3600, Oct 2018.

[6] S. Roy, J. Lee, and S. Baldi, "A new adaptive-robust design for time delay control under state-dependent stability condition," *IEEE Transactions on Control Systems Technology*, vol. 29, no. 1, pp. 420–427, 2021.

[7] ——, "A new continuous-time stability perspective of time-delay control: Introducing a state-dependent upper bound structure," *IEEE Control Systems Letters*, vol. 3, no. 2, pp. 475–480, April 2019.

[8] M. Pi, Y. Kang, C. Xu, G. Li, and Z. Li, "Adaptive time-delay balance control of biped robots," *IEEE Transactions on Industrial Electronics*, vol. 67, no. 4, pp. 2936–2944, 2020.

[9] Y. Jin, P. H. Chang, M. Jin, and D. G. Gweon, "Stability guaranteed time-delay control of manipulators using nonlinear damping and terminal sliding mode," *IEEE Transactions on Industrial Electronics*, vol. 60, no. 8, pp. 3304–3317, Aug 2013.

[10] M. Jin, S. H. Kang, P. H. Chang, and J. Lee, "Robust control of robot manipulators using inclusive and enhanced time delay control," *IEEE/ASME Transactions on Mechatronics*, vol. 22, no. 5, pp. 2141–2152, Oct 2017.

[11] Y. Wang, F. Yan, J. Chen, F. Ju, and B. Chen, "A new adaptive time-delay control scheme for cable-driven manipulators," *IEEE Transactions on Industrial Informatics*, vol. 15, no. 6, pp. 3469–3481, June 2019.

[12] J. Lee, N. Deshpande, D. G. Caldwell, and L. S. Mattos, "Microscale precision control of a computer-assisted transoral laser microsurgery system," *IEEE/ASME Transactions on Mechatronics*, vol. 25, no. 2, pp. 604–615, 2020.

[13] B. Brahmi, M. Saad, C. Ochoa-Luna, M. H. Rahman, and A. Brahmi, "Adaptive tracking control of an exoskeleton robot with uncertain dynamics based on estimated time-delay control," *IEEE/ASME Transactions on Mechatronics*, vol. 23, no. 2, pp. 575–585, April 2018.

[14] M. Jin, J. Lee, and K. K. Ahn, "Continuous nonsingular terminal sliding-mode control of shape memory alloy actuators using time delay estimation," *IEEE/ASME Transactions on Mechatronics*, vol. 20, no. 2, pp. 899–909, 2015.

[15] J. Kim, H. Choi, and J. Kim, "A robust motion control with antiwindup scheme for electromagnetic actuated microrobot using time-delay estimation," *IEEE/ASME Transactions on Mechatronics*, vol. 24, no. 3, pp. 1096–1105, 2019.

[16] B. Lu, Y. Fang, N. Sun, and X. Wang, "Antiswing control of offshore boom cranes with ship roll disturbances," *IEEE Transactions on Control Systems Technology*, vol. 26, no. 2, pp. 740–747, 2018.

[17] Y. Qian and Y. Fang, "Switching logic-based nonlinear feedback control of offshore ship-mounted tower cranes: A disturbance observer-based approach," *IEEE Transactions on Automation Science and Engineering*, vol. 16, no. 3, pp. 1125–1136, 2019.

[18] J. Kim, M. Jin, W. Choi, and J. Lee, "Discrete time delay control for hydraulic excavator motion control with terminal sliding mode control," *Mechatronics*, vol. 60, pp. 15 – 25, 2019.

[19] B. Della Corte, H. Andreasson, T. Stoyanov, and G. Grisetti, "Unified motion-based calibration of mobile multi-sensor platforms with time delay estimation," *IEEE Robotics and Automation Letters*, vol. 4, no. 2, pp. 902–909, April 2019.

[20] S. Roy, I. N. Kar, and J. Lee, "Toward position-only time-delayed control for uncertain Euler–Lagrange systems: Experiments on wheeled mobile robots," *IEEE Robotics and Automation Letters*, vol. 2, no. 4, pp. 1925–1932, Oct 2017.

[21] P. H. Chang, S.-H. Park, and J.-H. Lee, "A Reduced Order Time-Delay Control for Highly Simplified Brushless DC Motor," *Journal of Dynamic Systems, Measurement, and Control*, vol. 121, no. 3, pp. 556–560, 1999.

[22] D. Kim, K. Koh, G. Cho, and L. Zhang, "A robust impedance controller design for series elastic actuators using the singular perturbation theory," *IEEE/ASME Transactions on Mechatronics*, vol. 25, no. 1, pp. 164–174, 2020.

[23] Y. Wu, N. Sun, H. Chen, and Y. Fang, "Adaptive output feedback control for 5-dof varying-cable-length tower cranes with cargo mass estimation," *IEEE Transactions on Industrial Informatics*, pp. 1–1, 2020.

[24] T. Yang, N. Sun, H. Chen, and Y. Fang, "Observer-based nonlinear control for tower cranes suffering from uncertain friction and actuator constraints with experimental verification," *IEEE Transactions on Industrial Electronics*, pp. 1–1, 2020.

[25] Y. Fang, B. Ma, P. Wang, and X. Zhang, "A motion planning-based adaptive control method for an underactuated crane system," *IEEE Transactions on Control Systems Technology*, vol. 20, no. 1, pp. 241–248, Jan 2012.

[26] V. Sangwan and S. K. Agrawal, "Effects of viscous damping on differential flatness-based control for a class of under-actuated planar manipulators," *IEEE Control Systems Letters*, vol. 2, no. 1, pp. 67–72, Jan 2018.

[27] D. Invernizzi, M. Lovera, and L. Zaccarian, "Integral ISS-based cascade stabilization for vectored-thrust UAVs," *IEEE Control Systems Letters*, vol. 4, no. 1, pp. 43–48, Jan 2020.

[28] R. Skjetne, O. Smogeli, and T. I. Fossen, "Modeling, identification, and adaptive maneuvering of cybership II: A complete design with experiments," *IFAC Conference on Computer Applications in Marine Systems - CAMS, Ancona, Italy*, vol. 37, no. 10, pp. 203 – 208, 2004.

[29] R. Skjetne, T. I. Fossen, and P. V. Kokotović, "Adaptive maneuvering, with experiments, for a model ship in a marine control laboratory," *Automatica*, vol. 41, no. 2, pp. 289 – 298, 2005.

[30] A. P. Aguiar and J. P. Hespanha, "Trajectory-tracking and path-following of underactuated autonomous vehicles with parametric modeling uncertainty," *IEEE Transactions on Automatic Control*, vol. 52, no. 8, pp. 1362–1379, Aug 2007.

[31] A. Sintov, A. S. Morgan, A. Kimmel, A. M. Dollar, K. E. Bekris, and A. Boularias, "Learning a state transition model of an underactuated adaptive hand," *IEEE Robotics and Automation Letters*, vol. 4, no. 2, pp. 1287–1294, April 2019.

[32] R. Olfati-Saber, "Normal forms for underactuated mechanical systems with symmetry," *IEEE Transactions on Automatic Control*, vol. 47, no. 2, pp. 305–308, 2002.

[33] Y. Zhang, S. Li, and X. Liu, "Adaptive near-optimal control of uncertain systems with application to underactuated surface vessels," *IEEE Transactions on Control Systems Technology*, vol. 26, no. 4, pp. 1204–1218, July 2018.

[34] D. Pucci, F. Romano, and F. Nori, "Collocated adaptive control of underactuated mechanical systems," *IEEE Transactions on Robotics*, vol. 31, no. 6, pp. 1527–1536, Dec 2015.

[35] J. Huang, S. Ri, T. Fukuda, and Y. Wang, "A disturbance observer based sliding mode control for a class of underactuated robotic system with mismatched uncertainties," *IEEE Transactions on Automatic Control*, vol. 64, no. 6, pp. 2480–2487, 2018.

[36] B. Lu, Y. Fang, and N. Sun, "Continuous sliding mode control strategy for a class of nonlinear underactuated systems," *IEEE Transactions on Automatic Control*, vol. 63, no. 10, pp. 3471–3478, 2018.

[37] A. A. Paranjape, J. Guan, S. Chung, and M. Krstic, "Pde boundary control for flexible articulated wings on a robotic aircraft," *IEEE Transactions on Robotics*, vol. 29, no. 3, pp. 625–640, 2013.

[38] Y. Fan, Y. Cao, and T. Li, "Adaptive integral backstepping control for trajectory tracking of a quadrotor," in *2017 4th International Conference on Information, Cybernetics and Computational Social Systems (ICCSS)*, 2017, pp. 619–624.

[39] L. Zhang, C. Fu, X. Guo, Y. Bai, and Y. Tian, "Adaptive backstepping control algorithm for a rotorcraft disturbed by different wind," in *2017 6th Data Driven Control and Learning Systems (DDCLS)*, 2017, pp. 270–275.

[40] J. Wang, C. Wang, Y. Wei, and C. Zhang, "Three-dimensional path following of an underactuated auv based on neuro-adaptive command filtered backstepping control," *IEEE Access*, vol. 6, pp. 74 355–74 365, 2018.

[41] S. Kim, S. Choi, H. Kim, J. Shin, H. Shim, and H. J. Kim, "Robust control of an equipment-added multirotor using disturbance observer," *IEEE Transactions on Control Systems Technology*, vol. 26, no. 4, pp. 1524–1531, 2018.

[42] L. Liu, D. Wang, Z. Peng, T. Li, and C. L. P. Chen, "Cooperative path following ring-networked under-actuated autonomous surface vehicles: Algorithms and experimental results," *IEEE Transactions on Cybernetics*, vol. 50, no. 4, pp. 1519–1529, 2020.

[43] J. Svacha, J. Paulos, G. Loianno, and V. Kumar, "Imu-based inertia estimation for a quadrotor using newton-euler dynamics," *IEEE Robotics and Automation Letters*, vol. 5, no. 3, pp. 3861–3867, 2020.

[44] S. Thombre, Z. Zhao, H. Ramm-Schmidt, J. M. V. García, T. Malkamäki, S. Nikolskiy, T. Hammarberg, H. Nuortie, M. Z. H. Bhuiyan, S. Särkkä, and V. V. Lehtola, "Sensors and ai techniques for situational awareness in autonomous ships: A review," *IEEE Transactions on Intelligent Transportation Systems*, pp. 1–20, 2020.

[45] S. Roy, S. Baldi, and L. M. Fridman, "On adaptive sliding mode control without a priori bounded uncertainty," *Automatica*, vol. 111, p. 108650, 2020.

[46] D. Rohr, T. Stastny, S. Verling, and R. Siegwart, "Attitude and cruise control of a VTOL tiltwing UAV," *IEEE Robotics and Automation Letters*, vol. 4, no. 3, pp. 2683–2690, 2019.

[47] Y. Qin, W. Xu, A. Lee, and F. Zhang, "Gemini: A compact yet efficient bi-copter UAV for indoor applications," *IEEE Robotics and Automation Letters*, vol. 5, no. 2, pp. 3213–3220, 2020.

[48] F. Furrer, M. Burri, M. Achtelik, and R. Siegwart, *RotorS – A Modular Gazebo MAV Simulator Framework*, 01 2016, vol. 625, pp. 595–625.

[49] D. Mellinger, Q. Lindsey, M. Shomin, and V. Kumar, "Design, modeling, estimation and control for aerial grasping and manipulation," in *2011 IEEE/RSJ International Conference on Intelligent Robots and Systems*, 2011, pp. 2668–2673.

[50] D. Mellinger and V. Kumar, "Minimum snap trajectory generation and control for quadrotors," in *2011 IEEE International Conference on Robotics and Automation*. IEEE, 2011, pp. 2520–2525.

[51] S. Tang, V. Wüest, and V. Kumar, "Aggressive flight with suspended payloads using vision-based control," *IEEE Robotics and Automation Letters*, vol. 3, no. 2, pp. 1152–1159, 2018.

[52] K. Mohammadi, S. Sirouspour, and A. Grivani, "Control of multiple quad-copters with a cable-suspended payload subject to disturbances," *IEEE/ASME Transactions on Mechatronics*, 2020.

[53] G. Yu, D. Cabecinhas, R. Cunha, and C. Silvestre, "Nonlinear backstepping control of a quadrotor-slung load system," *IEEE/ASME Transactions on Mechatronics*, vol. 24, no. 5, pp. 2304–2315, 2019.

[54] Y. Shtessel, C. Edwards, L. Fridman, and A. Levant, *Sliding Mode Control and Observation,*. Birkhauser, Springer, New York, 2014.

Spandan Roy received the B.Tech. in Electronics and Communication engineering from Techno India (Salt Lake), West Bengal University of Technology, Kolkata, India, in 2011, the M.Tech. in Mechatronics from Academy of Scientific and Innovative Research, New Delhi, India, in 2013, and the Ph.D. in control and automation from Indian Institute of Technology Delhi, India, in 2018. He is currently Assistant Professor with Robotics Research Center, International Institute of Information Technology Hyderabad, India. Previously, he was Postdoc Researcher with Delft Center for System and Control, TU Delft, The Netherlands. His research interests include artificial delay based control, adaptive-robust control, switched systems and its applications in Euler–Lagrange systems.

Simone Baldi (M'14, SM'19) received the B.Sc. in electrical engineering, and the M.Sc. and Ph.D. in automatic control engineering from University of Florence, Italy, in 2005, 2007, and 2011. He is professor at School of Mathematics and School of Cyber Science and Engineering, Southeast University, with guest position at Delft Center for Systems and Control, TU Delft, where he was assistant professor. He was awarded outstanding reviewer for *Automatica* (2017). He is subject editor of *Int. Journal of Adaptive Control and Signal Processing*. His research interests are adaptive and learning systems with applications in unmanned vehicle systems.

Peng Li received the B.Sc. in Electronic Information Science and Technology from Hubei University of Science and Technology, China, in 2013, and the M.Tech. in Electronic Science and Technology from Wuhan University of Technology, China, in 2016. After that, he worked as a software engineer and he is currently pursuing the PhD in Cyber Science and Engineering at Southeast University, China. His research interests includes adaptive nonlinear control and its applications to unmanned vehicles.

Viswa Narayanan Sankaranarayanan received B. Tech. in Electronics and Instrumentation engineering from SRM University, Chennai, India, in 2015. Since then he worked as a software engineer at KPIT Technologies, Bangalore, India. He is currently pursuing MS by Research in Electronics and Communication Engineering at International Institute of Information Technology, Hyderabad, India. His research interests includes adaptive-robust control, switched systems and their applications in Euler-Lagrange systems.